Design of Teleoperated Surgical Instruments for Minimally Invasive Surgery

by

Akhil Jiten Madhani

B.S.M.E., University of California at Berkeley (1989)
S.M.M.E., Massachusetts Institute of Technology (1991)

Submitted to the Department of Mechanical Engineering
in partial fulfillment of the requirements for the degree of

Doctor of Philosophy

at the

MASSACHUSETTS INSTITUTE OF TECHNOLOGY

February 1998

Author . . . .
Department of Mechanical Engineering
September 15, 1997

Certified by . . . .
Dr. J. Kenneth Salisbury Jr., Thesis Supervisor
Principle Research Scientist, Mechanical Engineering, MIT

Accepted by . . . .
Professor Ain A. Sonin
Chair, Department Graduate Committee

Design of Teleoperated Surgical Instruments for Minimally Invasive Surgery

by

Akhil Jiten Madhani

Submitted to the Department of Mechanical Engineering
on September 15, 1997, in partial fulfillment of the
requirements for the degree of
Doctor of Philosophy

Abstract This thesis presents the design of two slave teleoperators for minimally invasive surgery. We demonstrate that it is possible to use teleoperation to solve several problems in current minimally invasive surgical practice. Specifically using teleoperation, we can eliminate geometrical transformations which the surgeon must overcome between tool motions and the camera image of the operating site, we can add dexterity and degrees of freedom over that which is currently available in MIS, and we can add a level of force feedback to allow surgeons to feel instrument tissue interactions.

We study these issues by designing two teleoeperator systems for minimally invasive telesurgery, the seven degree of freedom Silver Falcon and the eight degree of freedom Black Falcon. Both systems are used in conjunction with a Phantom™ Haptic Interface modified for use as a master. We achieve bilateral force-reflecting teleoperation in a system designed for MIS using good cable design principles but avoid the use of force sensors. Using macro-micro control and a corresponding wrist design, the dyamics of the system can be taken advantage of when designing a controller in order to reduce the effective slave endpoint inertia.

We found that the system had the appropriate kinematics and range of motion to allow suturing along aribitrarily oriented suture lines. Force reflection was however inadequate to help the suturing task. Force reflection is more useful during rigid contact tasks where force information is not available to the operator via visual cues. Tests were carried out using both the Phantom haptic interface and the Tool Handle (a scaled up version of the Phantom) as a master with each mounted with an instrumented gimbal and gripper.

Committee:

Dr. J. Kenneth Salisbury, Jr., Chairperson
Principle Research Scientist, Department of Mechanical Engineering, MIT

Dr. Joseph Rosen, M.D.
Associate Professor of Plastic Surgery, Department of Surgery, Dartmouth University

Dr. David Wallace
Associate Professor of Mechanical Engineering, MIT

Dr. Mandayam Srinivasan

Principle Research Scientist, Department of Electrical Engineering, MIT

Acknowledgments

Contents

List of Figures

Chapter 1

Introduction

Minimally Invasive Surgery (MIS) is the practice of performing surgery through small incisions or "ports" using specialized surgical instruments in order to reduce the size of incisions required to access human internal tissues during surgery. During conventional "open" surgery, the trauma created at the wound is typically greater than at the operating site. Therefore it is argued that procedures performed using MIS will have reduced bleeding, discomfort, patient recovery time, and cost.

However, MIS is technically more difficult for the surgeon. Surgeons must train extensively, and there still remains an increased risk of surgical complications which must be traded off against the opportunity for reduced morbidity. MIS is therefore limited to a number of relatively simple procedures such as cholecystecomy (gall bladder removal) for which there seems to be a consensus within the medical community that it is in fact beneficial, (NIH, 1993). Due in part to the changing landscape of medical reimbursement in the United States, there is a substantial push from medical payer organizations (insurance companies, health maintainance organizations, and hospitals) to introduce MIS to other procedures in order to reduce hospital stays and therefore costs. Recoveries are typically faster and less painful which also means patients are asking for these procedures.

In this thesis, I study and develop the design of a new class of surgical instruments which I hope will relieve the surgeon of key difficulties in current MIS practice. The goal is to perform current procedures more safely and with better results, but moreover to allow new MIS procedures to be performed which are currently impossible and by doing so to improve patient satisfaction and reduce the overall cost of these procedures.

As new technology is introduced we as a society must ascertain whether or not this new technology is beneficial. In medical care, we must weigh the quality of patient care against increased financial costs and possibly new risks. As an example, consider that there has recently been a great deal of interest in minimally invasive coronary artery bypass grafting, (Winslow, 1997), and several new approaches have been recently introduced. In Appendix A, we try to estimate whether these approaches will be beneficial by reviewing cost-effectiveness studies of several past cases: laparascopic cholecystectomy, coronary angioplasty, and open coronary artery bypass grafting. These studies may be a preview for the technology which we introduce in this thesis.

1.1 Current Minimally Invasive Surgery

Perhaps the most common forms of MIS is laparascopy, which is minimally invasive surgery within the abdominal cavity. Another common form is arthroscopy, minimally invasive surgery within the knee. A rapidly emerging field is MIS cardiac surgery for coronary artery bypass graft surgery (CABG). Others are being named as they are developed with the prefix referring to the body cavity under investigation (hysteroscopy, sinoscopy, pelviscopy, etc.) During laparascopy, a patient's abdomen is insufflated with CO_2, and cannulas (essentially metal tubes) with pneumatic check valves are passed through small (approximately 1-2 cm) incisions to provide entry ports for laparascopic surgical instruments.

The instruments include an endoscope for viewing the surgical site (a CCD camera/lens combination with a slender shaft), and tools such as needle-holders, graspers, scissors, clamps, staplers, and electrocauteries. The instruments differ from conventional instruments in that the working end is separated from its handle by an approximately 30 cm long, 4-13 mm diameter shaft.

The surgeon passes these instruments through the cannula and manipulates them inside the abdomen by sliding them in and out, rotating them about their long axis and pivoting them about centers of rotation defined roughly by their incision site in the abdominal wall. Typically a one degree of freedom (DOF) device (gripper, scissors, etc.) can be actuated with a handle via a tension rod running the length of the instrument. The surgeon monitors the procedure by means of a television monitor which displays the abdominal worksite image provided by the laparascoic camera.

There are several disadvantages to current MIS technology.

1. Visualization of the surgical site is reduced. The operating site is viewed on an upright, two-dimensional video monitor placed somewhere in the operating room. The surgeon is deprived of three-dimensional depth cues and must learn the appropriate geometrical transformations to properly correlate hand motions to tool tip motions.

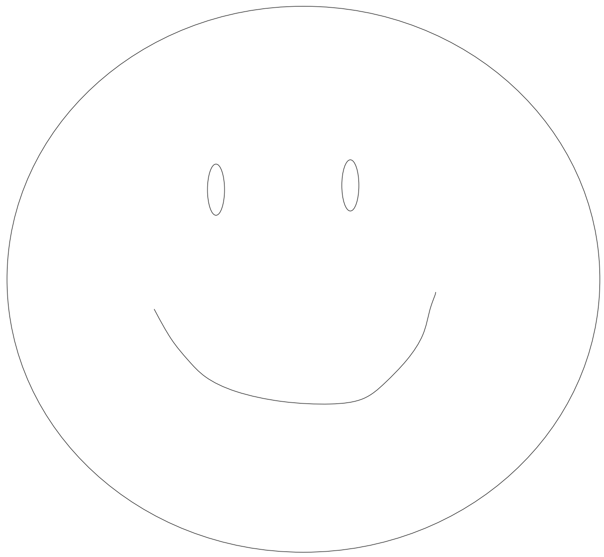

Figure 1-1: A typical MIS instrument, the Ethicon Disposable Babcock

2. The surgeon's ability to orient the instrument tip is reduced. The incision point/cannula restricts the motions of the instrument from six DOF to four. As a result, the surgeon can no longer approach tissue from an arbitrary angle and is often forced to use secondary instruments to manipulate the tissue in order to access it properly or to use additional incision sites. Suturing become particularly difficult.

3. The surgeon's ability to feel the instrument/tissue interaction is nearly eliminated. The instruments are somewhat constrained from rotating and sliding within the cannula due to sliding friction from the air seal, and the body wall constrains pivoting motions of the instrument shaft. The mechanical advantage designed into MIS instruments reduces the ability to feel grasping/cutting forces at the handle.

Despite surgeons' considerable skill and ability to work within the constraints of current MIS technology, the expansion of minimally invasive medical practice remains limited by the lack of dexterity with which surgeons can operate while using current MIS instruments.

1.2 Teleoperators as the next step in MIS

We propose *teleoperation* as a solution to this problem. Our goal is to improve the dexterity possible during MIS procedures through the use of *teleoperated surgical instruments* and in certain cases to improve the surgeon's dexterity over that when using conventional instruments during open surgery.

1.2.1 What are Teleoperators?

Teleoperators are machines designed to allow a user to manipulate objects in a location remote from his own. They have historically been used to allow people to work remotely in dangerous or inaccessible environments such as nuclear reactors, the deep sea, and space.

A teleoperator consists of two mechanical systems of linkages, a master manipulator and a slave manipulator, (typically arms with grippers on the ends). These are connected either (a) mechanically, for example by cables or linkages, or (b) by servoactuating both the master and slave (e.g. using electric motors) and controlling each manipulators via computer. Motions are transmitted from the master to the slave so the user may manipulate the slave environment remotely.

There are many variations on this basic idea including the addition of other sensory modalities and inputs. For example sound, tactile stimulus and forces can be transmitted from the slave environment to the user. In particular, it is useful to transmit motions and forces from the master to the slave, and motions and forces from the slave back to the master. This is known as bilateral force-reflecting teleoperation.

1.2.2 Teleoperators used for MIS

What follows is our vision for how teleoperators will be used for MIS, see Figure 1-2. The surgeon will sit at a console where they will be provided with a three-dimensional image of the operating site. The surgeon will simultaneously manipulate a master manipulators which controls a slave manipulator. The distal end of the slave will pass through a cannula in the body wall in order to access the surgical site. Most likely, the surgeon would use two masters to control two slaves so that he might work with both hands. Different quick-release slave end-effectors would be available to duplicate the surgeon's current array of instruments such as needle drivers, tissue graspers, and clamps.

The surgeon will have several advantages when using such a system:

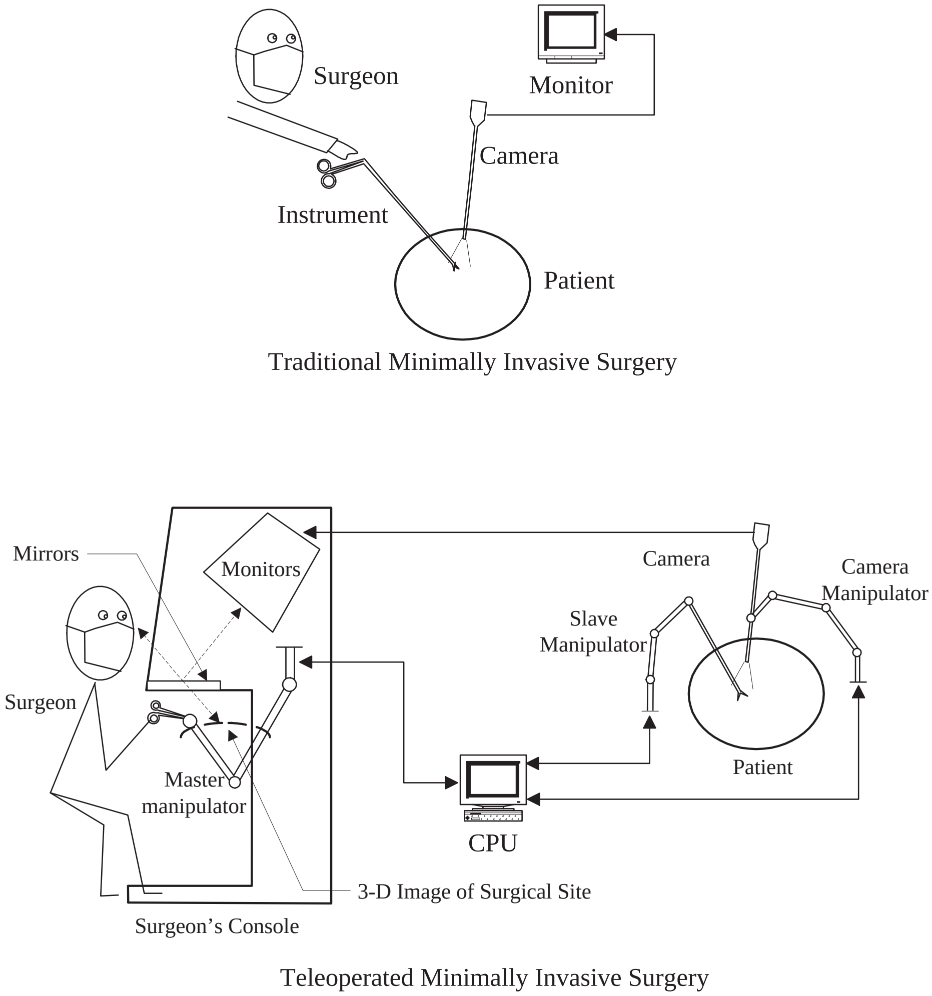

Figure 1-2: In MIS Telesurgery, the surgeon will sit at a *surgeon's console* within the OR. He will remotely control a *surgical slave manipulator* and a *camera slave manipulator* using a *master manipulator*. Most likely, he will control two surgical slaves using two surgical masters. The monitors and console will be arranged such that his hand and wrist motions are similar to those used during open procedures. The slave must be designed with sufficient degrees of freedom to perform these motions. The goal is to create the illusion, with the accompanying increase in manual dexterity, that he *is* performing open surgery. The door is opened to enhanced modes of surgery: motion scaling, force scaling, visual and haptic overlays to improve dexterity over that of open surgery.

1. By viewing a three-dimensional image of the slave instruments geometrically aligned with his own hands which are manipulating the master manipulators, the illusion is created for the surgeon that he in fact directly manipulating the slave instruments. The surgeons hands appear connected to the actual instruments which he views, since hand motions are directly correlated to the instrument motions as they are when a surgeon manipulates conventional instruments during open procedures. This illusion was created very successfully by SRI with their open surgical teleoperation system, (Hill et al., 1994).

2. We will show that the slave can be designed with additional degrees of freedom by adding additional "wrist" joints beyond the cannula. It is easier for the designer to do this than in the case of hand-held instruments, because the joints are servoactuated. The endpoint mobility of the instruments can then be increased to six degrees of freedom to provide greater access to the tissue and hence greater dexterity. The goal is for the surgeon to be able to suture naturally, that is in the same fashion as when performing open surgery.

3. Finally, if accurate force and tactile information can be transferred back to the surgeon, this will improve the illusion by making him feel as though he were manipulating the surgical instruments or the tissue itself directly by hand. We will find that this goal, in particular in a system with 7 or 8 degrees of freedom, is by far the most difficult.

Success in these areas would give back to the surgeon dexterity which was lost when procedures were converted from open to minimally-invasive, and would expand the type and number of MIS procedures possible. But the door to additional capabilities is opened. Consider that:

1. Motions and forces could be scaled. For example, if a 1 mm slave motion is made to correspond to a 5 mm master motion and if the image of the operating site is magnified correspondingly, it will appear to the surgeon that the operating site has been enlarged, therebey allowing finer absolute motions. 1 mm vessels would appear to be 5 mm vessels. Also, if forces between the instrument and tissue are scaled up and accuarately transferred to the surgeon, the illusion will be even more convincing.

2. Semi-autonomous behaviors could be introduced into the slave manipulators and the camera, if it were mounted on a seperate controllable arm. For example, the camera and slave manipulators could be programmed to track moving tissue such as a beating heart. In the case of beating heart surgery, the heart would now appear stationary, thus allowing the surgeon to perform delicate tasks such

as suturing without having to stop the heart from beating and using cardio pulmonary bypass as in conventional heart surgery.

3. Graphic overlays could be placed in the surgical workspace to aid visualization of the operating site. For example, if a liver tumor must be removed but is viewable only using MRI, an image of the tumor could be overlayed on the surgeon's actual image of the liver so that he would know where to operate. This concept has been used sucessfully in brain surgery (Grimson et al., 1996), where a seperate 2-D monitor is placed in the operating room to guide the surgeon towards brain tumors.

4. Haptic overlays could be placed into the surgical workspace. In this case, virtual objects would be placed within the workspace to help guide the surgeon by feel. For example, since the master manipulator will be actuated, we could apply forces which like a funnel would guide the surgeon towards a tumor. Or if some part of the anatomy such as a nerve bundle must be avoided, a force field could be placed around the nerve bundle so that the surgeon cannot cut it with the slave manipulator.

We refer to the overall package as *enhanced teleoperation*. All of these areas present a variety of exciting research topics in the next generation of surgery, in teleoperation, and in haptic and force feedback devices.

1.3 Thesis Scope and Overview

This thesis concentrates on teleoperator slave design. Control methods are studied for such systems in order to better design them. We present designs of two force-reflecting teleoperators for minimally invasive telesurgery, the Silver Falcon and the Black Falcon. We discuss the important issues involved with making such systems work from both controls and mechanisms perspectives, and focus in particular on design for force reflection. Our goal is not to use these systems on humans, thereby relieving us of certain safety, sterilization, and tool interchangeability requirements. These issues are kept in mind, however, in particular during our second design, to allow future extension to human surgical practice.

1.3.1 The Silver Falcon Telesurgery Slave

Our first system is called the Silver Falcon and is described in Chapter 5. This is a seven degree of freedom teleoperator slave which consists of two major subsystems, a wrist unit and a base positioner. The wrist unit incorporates five motors to actuate a small three degree of freedom wrist and gripper mechanism which is placed at the end of a long slender shaft. This is the instrument shaft designed to pass through an incision into the patient. The wrist unit also rotates the shaft about its long axis and controls insertion of the shaft into the patient.

The second subsystem is a two degree of freedom base positioner which orients the wrist unit in pitch and in yaw about the incision point. It is designed to keep one point on the shaft stationary and coincident with the incision point.

This system was connected via a controller to a Phantom Haptic Interface which we modified to allow us to use it as a master manipulator for our slaves. This complete master/slave system allowed us to prove that the concept of macro-micro control was feasible when used to enable force reflection on a full master/slave system designed for minimally invasive surgery. It also showed us that our basic approach of using a small dextrous wrist coupled to a larger positioning mechanism could be effective for surgery and would allow us to perform intricate tasks such as suturing.

There were a number of areas where the Silver Falcon was limited however. We found that the wrist kinematics allowed us to use macro-micro control in only two out of three directions meaning that there was always one direction in which the surgeon could not feel forces. Obviously we would like the surgeon to feel forces in all three directions equally well. There were also practical issues such as excessive structural flexibility, insufficient base servo performance, and the lack of sufficient grip strength to hold needles securely. Finally the wrist was designed as an integral part of the system and is not interchangable with other instruments or sterilizable. All of these are important issues if we intend to understand minimally invasive telesurgery in an actual operating room environment.

1.3.2 The Black Falcon Telesurgery Slave

Our second telesurgical slave is called the Black Falcon, and is desribed in Chapter 6. This eight degree of freedom system is structurally stiffer and considerably stronger in terms of actuator capacity. The system is counterbalanced for safety by placing all of its actuators at its base and using cable transmissions to actuate the wrist and gripper. This also allows the wrist unit to be detatchable to allow future development of wrist-units which perform other functions, such as cutting, grasping tissue instead of needles, and cauterizing. This basic concept also allows the actual portion of the instrument which enters the body to be sterilized. The wrist was redesigned with an additional degree of freedom to allow macro-micro control in all three linear degrees of freedom with the goal of allowing forces to be felt equally well in all three directions.

We found that the system had the appropriate kinematics and range of motion to allow suturing along aribitrarily oriented suture lines. Force reflection was however inadequate to help the suturing task. Force reflection is more useful during rigid contact tasks where force information is not available to the operator via visual cues.

During the course of this work and experimentation with both the Silver Falcon and the Black Falcon, we learned a great deal about how a master should be designed for surgery. While we did not design a new master as part of this work, some of our observations have been recorded in Chapter 7 as this is logically on the critical path towards developing a complete and more refined system for minimally invasive telesurgery.

1.3.3 Outline

Chapter 2 introduces basic teleoperator control and discusses physical hardware limitations which affect the performance of robotic systes. We discuss past work in teleoperator hardware, haptic interfaces, and telesurgery systems.

In Chapter 3 we describe several ways to control a system with widely different base and end-effector inertias. This chapter demonstrates the effects of different types of controllers on a three degree of freedom master/slave testbed, and shows that a Jacobian Inverse control takes advantage of this inertia difference to improve performance.

Chapter 4 outlines our view of the relavant objectives and constraints in the design of a slave manipulator for minimally invasive surgery.

Chapter 5 gives a detailed description of our first teleoperator design, performance results and describe areas for improvement. Chapter 6 addresses these issues by presenting the design of a new teleoperator slave, the Black Falcon, and performance results.

Finally, In Chapter 7, we summarize our work and present further areas for improvement and future research with this system.

Chapter 2

Background

In this chapter we first discuss basic force reflecting teleoperator control. We then discuss several methods generally used to control forces at the endpoints of manipulators. We discuss some interesting past telemanipulator designs, haptic interface designs, and telesurgical systems.

2.1 Basic Force Reflecting Teleoperation

Consider a master manipulator and a slave manipulator, each with its own sensors, actuators, power supplies and amplifiers. Controlling each manipulator is a computer which reads sensor values from each and which commands actuator inputs based on a controller operating on the computer. Using this chain of elements, as shown in Figure 2-1 the human operator can interact with the environment. In our case, this will be a surgeon interacting with tissues at the surgical site.

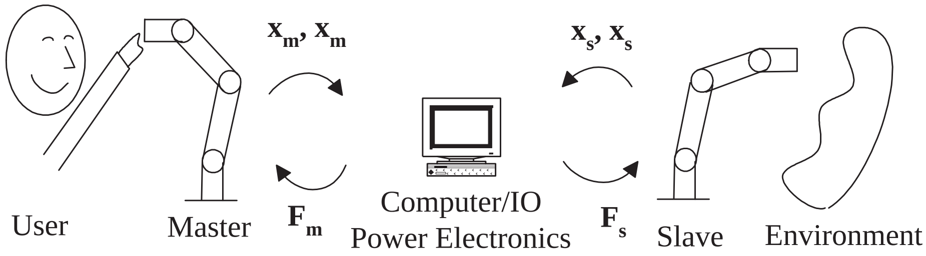

Figure 2-1: A basic teleoperator consists of a master, slave, and associated computer and electronic hardware to control each.

In our work, we limit ourselves to force feedback and forego use of other haptic modalities. In particular, we do not consider the use of direct tactile feedback. For example, tactile stimulus may be imparted to the user via direct stimulation of skin cutaneous sensors via devices which produce pressure maps across the fingertips, or via non-directional vibration sources. (Kontarinis, 1995), for example, studies vibration and shape feedback specifically for telemanipulation. Often, teleoperators are used to manipulate objects from a large distance introducing a communiations link with time delay between the master and slave manipulators. We will not consider communication delays in our system.

Below we describe basic position based bilateral force reflecting teleoperator control. The discussion is based on (Niemeyer, 1996).

2.1.1 Basic Teleoperator

The dynamics of the master and slave may be expressed as

$$H_m(\mathbf{q}_m)\ddot{\mathbf{q}}_m + C_m(\mathbf{q}_m, \dot{\mathbf{q}}_m)\dot{\mathbf{q}}_m + G_m(\mathbf{q}_m) = -\boldsymbol{\tau}_m \tag{2.1a}$$

$$H_s(\mathbf{q}_s)\ddot{\mathbf{q}}_s + C_s(\mathbf{q}_s, \dot{\mathbf{q}}_s)\dot{\mathbf{q}}_s + G_s(\mathbf{q}_s) = \boldsymbol{\tau}_s \tag{2.1b}$$

where $\mathbf{q}$ is the vector of joint positions, H is the inertia matrix, $C\dot{\mathbf{q}}$ are coriolis torques, G are gravitational torques, and $\boldsymbol{\tau}$ are motor torques, (Asada and Slotine, 1986)

To control the system, we compensate for gravity by calculating and feeding forward gravitational torques, and use P.D. feedback to force tracking between the master and slave joints.

$$\boldsymbol{\tau}_m = -G_m(\mathbf{q}_m) + \boldsymbol{\tau}_{PD} \tag{2.2a}$$

$$\boldsymbol{\tau}_s = -G_m(\mathbf{q}_s) - \boldsymbol{\tau}_{PD} \tag{2.2b}$$

$$\boldsymbol{\tau}_{PD} = -K(\mathbf{q}_m - \mathbf{q}_s) - B(\dot{\mathbf{q}}_m - \dot{\mathbf{q}}_s) \tag{2.2c}$$

If the feedback gains K and B are symmetric positive definite matrices, then the master and slave will appear to be connected via a spring and damper. Figure 2-2 shows the mechanical equivalent for a one degree of freedom system.

2.1.2 Jacobian Transpose Cartesian Control

The above controller assumes that we are using a kinematically similar master and slave. If this is not the case, then the most straightforward method of cartesian control

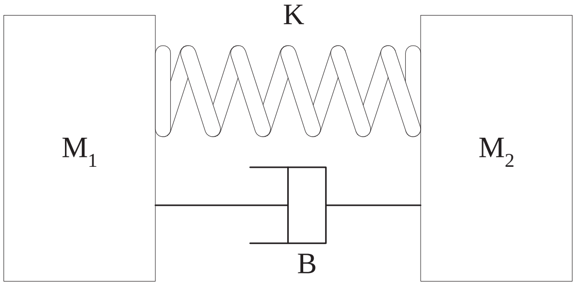

Figure 2-2: The basic teleoperator mimicks two inertias connected via a spring and damper in the one degree of freedom case.

is to implement tracking between the endpoints of each manipulator. To do this, we calculate the endpoint position $\mathbf{x}$ and endpoint velocity $\dot{\mathbf{x}}$ using the manipulator geometry. We then apply a P.D. controller to find the resulting endpoint forces and torques, $\mathbf{F}$. These are then converted to joint torques $\boldsymbol{\tau}$ and commanded to the master and slave motors.

Endpoint velocities are calculated as follows, where J is typically referred to as the manipulator Jacobian:

$$\dot{\mathbf{x}}_m = J_m(\mathbf{q}_m)\dot{\mathbf{q}}_m \quad (2.3a)$$
$$\dot{\mathbf{x}}_s = J_s(\mathbf{q}_s)\dot{\mathbf{q}}_s \quad (2.3b)$$

The joint P.D. is replaced with a cartesian version:

$$\mathbf{F}_{PD} = K(\mathbf{x}_m - \mathbf{x}_s) + B(\dot{\mathbf{x}}_m - \dot{\mathbf{x}}_s) \quad (2.4a)$$
$$\mathbf{F}_m = \mathbf{F}_{PD} \quad (2.4b)$$
$$\mathbf{F}_s = \mathbf{F}_{PD} \quad (2.4c)$$

The resulting joint torques are then calculated:

$$\boldsymbol{\tau}_m = J_m^T(\mathbf{q}_m)\mathbf{F}_m + G_m(\mathbf{q}_m) \quad (2.5a)$$
$$\boldsymbol{\tau}_s = J_s^T(\mathbf{q}_s)\mathbf{F}_s + G_s(\mathbf{q}_s) \quad (2.5b)$$

Figure 2-3 shows the system in block diagram form with the kinematic transformations included.

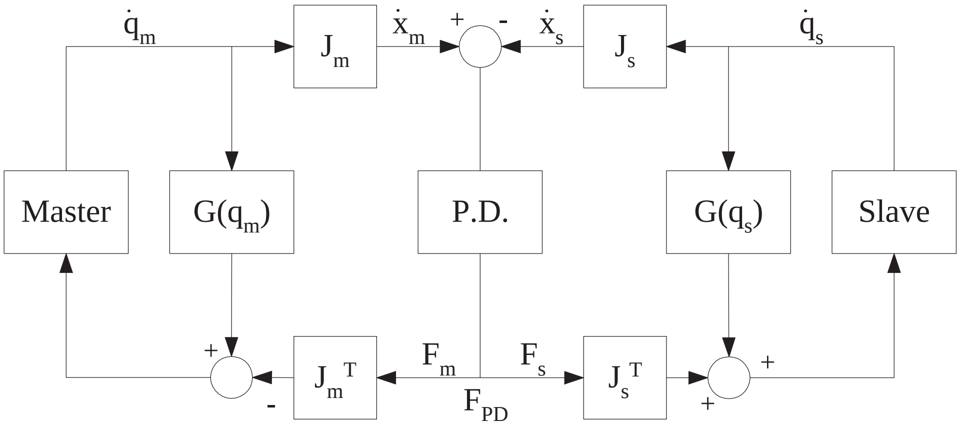

Figure 2-3: Both master and slave robots are gravity compensated, transformed into a cartesian domain, then connected via a P.D. controller mimicking a spring and damper.

2.1.3 Scaling

One way in which we can change the user's perception of the environment is to scale positions and forces betweeen the master and the slave. We may introduce scaling into the above system in order to change the size of relative motions and to amplify forces between the master and slave. This is done by introducing the scale factors η_P and η_F as shown in Figure 2-4.

Scaling will effect the users perception of the environment and of the teleoerpator:

- $\eta_F > 1, \eta_P = 1$ Forces are scaled up from the slave to the master. Velocities remain one to one. In this case, the user will feel an increases slave/environment impedance. Objects in the environment will therefore feel stiffer and heavier. This will make transitions between freespace and contact to feel crisper and more noticable. However, the dyanamics of the slave, such as friction and inertia, will also be amplified and felt by the user. As a result, these undesirable elements will have to be very low in the slave if eta_F scaling is to be large. Conversely, the environment will feel a reduced master/user impedance. The environment will more easily backdrive the master and human operator.

- $\eta_F < 1, \eta_P = 1$ Forces are scaled down from the slave to the master. Velocities remain one to one. The situtation is inverse of the previous case. Note that as long as $\eta_F > 0$, some level of force reflection will exist.

- $\eta_P > 1, \eta_F = 1$ Positions are scaled up from the slave to the master. Forces re-

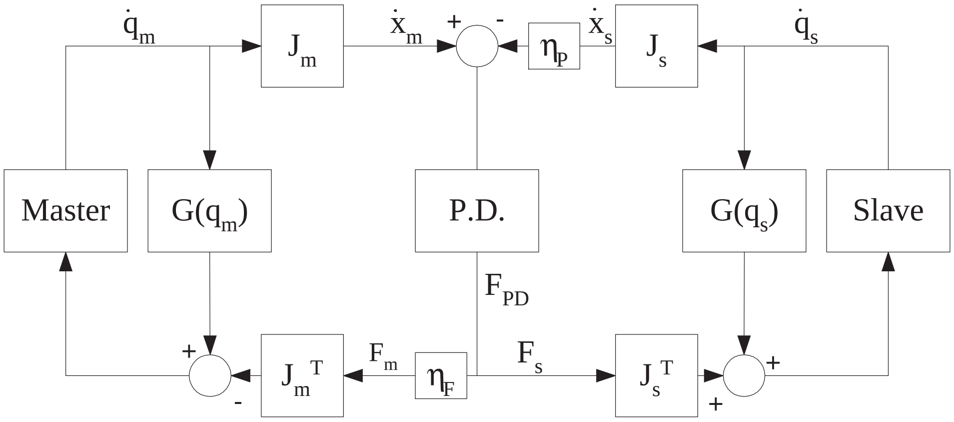

Figure 2-4: Both master and slave robots are gravity compensated, transformed into a cartesian domain, then connected via a P.D. controller mimicking a spring and damper. Scaling is included.

main one to one. In this case, motions made by the human operator are reduced, making fine motions easier to perform. Steady state forces will be equal at the master and slave. Therefore, the user will feel a decrease in slave/environment impedance. Transitions made between freespace and contact will feel softer softened and will be more difficult to distinguish.

- $\eta_P < 1, \eta_F = 1$ Positions are scaled down from the slave to the master. Forces remain one to one. Fine motion control now becomes more difficult, since errors in the users motions will be amplified. But the slave/environment impedance increases as felt by the master/user so that contacts will be easier to distinguish.

2.2 Limitations

Theoretically, if the inertia of the slave and master were zero, and the P.D. gains were infinite, the system would be transparent. In other words, forces and motions at the slave and master would be identical. Or if scaling were implemented, forces and motions would be exact scaled versions of one another. In a real system, of course, infinite gains and massless linkages are impossible. In what follows, we discuss several real world limitations.

2.2.1 Relation of Stiffness to Inertia

Consider again our model for a one degree of freedom teleoperator shown in Figure 2-2. The dynamics can be written as:

$$m_1\ddot{x}_1 = K(x_2 - x_1) + B(\dot{x}_2 - \dot{x}_1) \tag{2.6}$$
$$m_2\ddot{x}_2 = -K(x_2 - x_1) - B(\dot{x}_2 - \dot{x}_1) \tag{2.7}$$

Or in Laplace notation where s is the Laplace operator:

$$m_1 x_1 s^2 = K(x_2 - x_1) + B(x_2 - x_1)s \tag{2.8}$$
$$m_2 x_2 s^2 = -K(x_2 - x_1) - B(x_2 - x_1)s \tag{2.9}$$

Which simplifies to:

$$s^2(m_1 m_2 s^2 + (m1 + m2)Bs + (m_1 + m_2)K)x_1 = 0 \tag{2.10}$$
$$s^2(m_1 m_2 s^2 + (m1 + m2)Bs + (m_1 + m_2)K)x_2 = 0 \tag{2.11}$$

The natural frequency is then:

$$\omega_n = \sqrt{\frac{K}{\frac{m_1 m_2}{m_1 + m_2}}} = \sqrt{\frac{K}{M_{eff}}} \tag{2.12}$$

where M_{eff} is an effective mass.

In practice the system will always have a bandwidth limitation, ω_b. To ensure stability, we should impose a frequency limit λ below this limitation, say at $\lambda = \omega_b/5$. Typically, ω_b is caused by the finite servo rate of a digital controller, or the bandwidth of motor amplifiers. As a result, we have the following tradeoff. On one hand, we desire a system with low inertia, so that the teleoperator feels light to the human operator. For a given effective mass M_{eff}, however, our stiffness is then limited by:

$$K < \lambda^2 M \tag{2.13}$$

On the other hand, if we desire a certain stiffness, K, then the effective mass, M_{eff} is limited by:

$$M_{eff} > \frac{K}{\lambda^2} \tag{2.14}$$

Stated otherwise, we can either (a) design the system to have a high inertia in order to make the connection between the master and slave stiff, or (b) design the system to have low inertia, but have a low stiffness as a result. In practice we comprimise in order to have sufficiently high stiffness and sufficiently low inertia to make the system usable.

2.2.2 Position Measurement

There are many effects which contribute to a system bandwidth limit. Typically each gain K and B will be limited for different reasons which make the situation a bit more complicated. Below we give a simple rule of thumb relating digital position measurement resolution and the gain K which can be achieved.

Digital encoders are very convenient for measuring joint positions. It is typical to differentiate this measurement to infer joint velocities because velocity measuring devices (tachometers) are bulky and costly. Furthermore, digital encoders are relatively immune to outside sources of noise and add very little mass and no friction to a motor when mounted directly to a motor shaft. They are not limited in the number of revolutions which can be measured, and electronics to read encoders are common and straightforward. These are all advantages over using analog potentiometers. They are of course digital, and this causes several problems.

Digital position measurement limits the servo stiffness (position gain k) which can be implemented. Consider the position term for a one degree of freedom P.D. controller:

$$F = -K(x - x_d) \tag{2.15}$$

Where the actual position is x, the desired position is x_d, the measured position is x_m, the controller force is F, and the position resolution is Δ. If the position sensing is digital, the resulting forces are form a staircase as shown in Figure 2-5. In nearly all cases, $x_d \neq x_m$. Therfore $F \neq 0$. The largest F can be is $K\Delta$. In the abscence of friction, the system will continuously bounce between steps without settling to a fixed value.

In the presence of friction, it would seem the energy would approach zero. However, time delay induced by finite servo rate provides a mechanism to add energy to the limit cycle. Consider Figure 2-6. The dotted line shows the path of a system in a one resolution step limit cycle. If we start at the upper left of the loop, labelled 1, the controller pushes the system to the right with a force of, in this case, $K\Delta/2$. At 2, the force should drop to $-K\Delta/2$, however due to the time delay the force is maintained until 3. The same effect is repeated in the other direction. The area of the loop represents the energy added during each cycle.

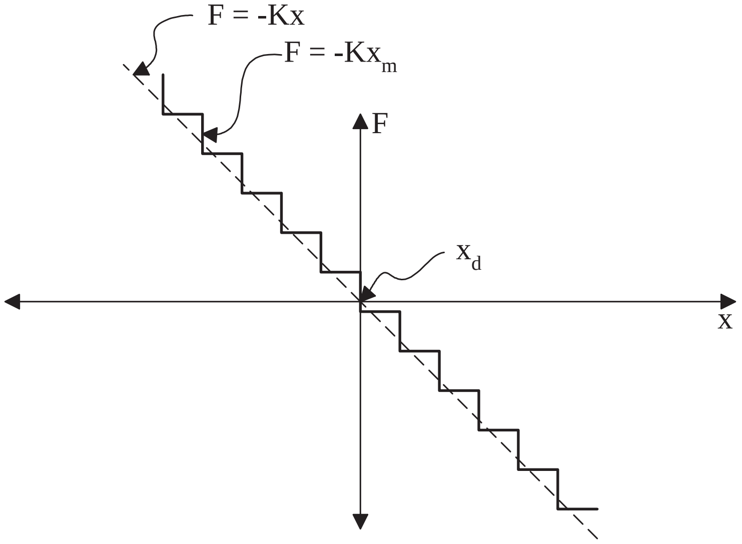

Figure 2-5: Instead of producing a straight line force output, a staircase is produced instead.

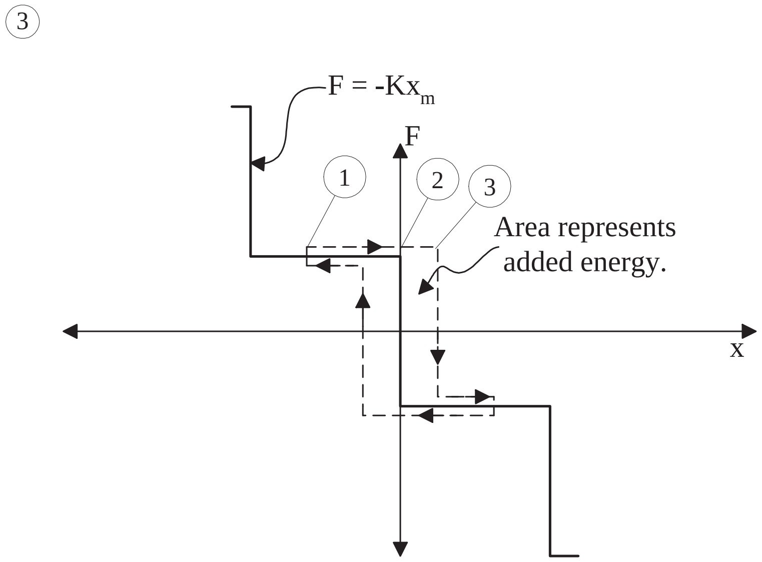

Figure 2-6: Time delay adds what looks like hysteresis to add energy to the limit cycle.

In practice, while it is usually beneficial to reduce friction in our mechanisms and transmissions, a little static friction helps with this problem. In particular, if the static friction level, F_f is greater than the force step $K\Delta$, then the limit cycle cannot start. Then, given our encoder resolution, and static friction, our gain is limited by:

$$K < \frac{F_f}{\Delta} \tag{2.16}$$

Increasing encoder resolution is obviously a more attractive solution over increasing static friction.

2.2.3 Velocity Estimation

Any time a position signal is differentiated in order to estimate velocity, a certain amount of "noise" will be added to the signal. Typically, we filter the velocity signal digitally in order to avoid injecting this noise into the system. The filter cutoff must be kept above the position servo bandwidth however to avoid adding lag to the control system.

2.3 Methods of Force Control

The statement that:

$$\boldsymbol{\tau} = J^T \mathbf{F}$$

makes several assumptions. First, it assumes there are no dynamics (friction and inertia) between the joint torques $\boldsymbol{\tau}$ and the manipulator endpoint where the force $\mathbf{F}$ is applied, that is, it is a statement of statics. Second, it presumes that the we are able to effectively command joint torques $\boldsymbol{\tau}$.

In fact, the art of manipulator design and control is largely concerned with addressing manipulator and actuator dynamics. Force control in particular is concerned with accurately generating interaction forces between the endpoint of a manipulator and its environment. Below we discuss just a few methods by which this has been tried. We emphasise that the environment of the master is the human operator. As a result we must understand how humans perceive forces. We will disuss this briefly below in section 2.6.

2.3.1 Commanded Motor Currents

The simplest form of manipulator endpoint force control is in fact to command motor currents open loop, and therefore to rely on the statement $\boldsymbol{\tau} = J^T\mathbf{F}$. We may be able to command joint torques in this way with a Lorentz force actuator such as a D.C. electric motor because torque is typically proportional to input current, and because we can command current using servo amplifiers which operate closed loop. The quality of the output force depends on the quality of the actuator. We are limited (as always) by amplifier bandwidth, and friction in the motor bearings and brushes. If a brushless motor is used with electronic commutation, the limit is typically in the electronics. The controller can introduce cogging even if the motor rotor intrinsically has none, (Paul, 1987), (Levin, 1990).

This approach forces us to design transmissions with low friction and to design manipulators with low inertia. While we may be able to design a large system with low friction, it is often impossible to design one with low inertia given structural considerations.

On the other hand, the approach is stable and will feel smooth (subject to the quality of the actuator), since no extraneous control system exists to add vibrations. This may seem like a small benefit, but when considering that a human will be directly interacting with the system, these benefits can be substantial.

2.3.2 Basic Closed Loop Force Control

Another common approach is to close a force control loop about a manipulator between a force sensor or sensors and the actuators. In colocated force control, a force sensor is placed very near the motor in an effort to minimize the dynamics between the force sensor and actuator. The goal is to make the motor/sensor appear as a perfect torque source. If motors were perfect Lorenz devices, this would be unnecessary, but in the presence of brush friction or non-ideal electronics, the sensor can be used to hide these unwanted dynamics. (Paul, 1987) used a torque sensor on the output of a brushless d.c. servomotor in order to control out ripple induced by the motor controller caused by imperfect electronic commutation. He concluded that the best way to compensate was to use feedforward compensation because the disturbances were position dependent and could be effectively mapped out with much less mechanical complexity.

(Levin, 1990) designed a reaction torque sensor into a housing custom designed for a framelss brushless d.c. torque motor. He found that with such a design he could achieve 200 Hz to 300 Hz bandwidths when commanding a step response in torque.

A major problem was eliminating noise picked up by the sensors generated by the motor's PWM servo amplifiers. This was eventually solved using hardware and software filters. Transmission dynamics, distal from the motor, cannot be compensated for with such a system, so that transmission design is still an important issue.

In a non-colocated arrangement, the sensor is placed near the end of a robot, separated from the motor by the linkages and transmissions that make up the robot. The difference is a matter of degree. More dynamics are introduced between the actuator and sensor, and kinematic transformations are involved in mapping endpoint force/torques onto the joints (J^T). Also, dynamic feedforward elements have been used to cancel manipulator dynamics. The goal is again to use the controller to hide these dynamics so that the entire robot appears to be a perfect force/torque source. This of course becomes increasingly difficult as the dynamics increase.

Examples can be found in (Mason and J. Kenneth Salisbury, 1985) where strain gage based tendon tension sensors are used to hide friction in cable conduits used in the Salisbury (NASA/JPL) Hand. Force control and the stability problems involved have been discussed by (Eppinger, 1988), (Whitney, 1985), (Kazerooni, 1985), (An, 1986), (Colgate and Hogan, 1989), (Volpe and Khosla, 1992), and others. Numerous other examples exist.

(Pratt and Williamson, 1995) gives another example of using a force sensor on the output of a motor to control output torques. This is a semi non-colocated arrangement where the output sensor is a steel torsional spring mounted with strain gages within each joint distal of a combination planetary gear/cable drive speed reduction used with each motor. The spring adds a substantial compliance to the system, but this was one of the goals in this case, as the system is typically run in a joint compliance control mode with soft positioning gains. The compliance of the force sensor has the advantage that it shields the planetary gear reductions which they use from external shock loads.

2.3.3 Parallel-Coupled Micro-Macro Control

(Morrell, 1996) pursues the idea of using two motors coupled in parallel to drive a load. The goal is to increase the ratio of maximum to minimum controllable force, a measure known as the dynamic range, over that of either actuator used individually. Figure 2-7 shows the concept. Because a flexible transmission is used to couple the macro motor to the load, its bandwidth in applying forces is limited by its position control bandwidth, that is how quickly it can produce a desired deflection in the flexible transmission. It can, however, apply large torques. The micro motor, on the other hand, will typically have a high bandwidth, but it can only apply only small

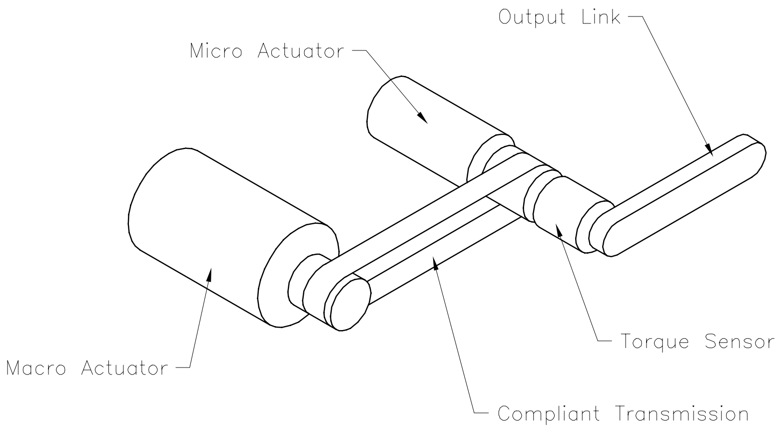

Figure 2-7: Parallel-coupled micro-macro control uses two actuators connected in parallel via a flexible transmission. A force sensor is required to sense the sum of the torques output by each actuator.

forces. At the output, torque must be sensed and fed back to the controller to allow the micro motor to compensate for disturbances introduced by the macro motor. If the motors, transmission stiffness, and controller are selected and designed properly, the advantages of each motor can be capitalized upon.

2.3.4 Series-Coupled Macro-Micro Control

(Sharon, 1988) studied the idea of coupling two manipulators in series, with one grounded on the other. The base manipulator (macro manipulator) is presumed to be larger and potentially flexible, but has a large range of motion. The distal manipulator (micro manipulator) is presumed to be smaller and have a higher position servo bandwidth. It is assumed that absolute endpoint position measurement of the tip of the macro-micro system is available. Figure 2-8 shows a model used for the study. The results were confirmed on a one degree of freedom macro-micro manipulator. The macro manipulator consisted of a d.c. electric motor with a cable reduction and a flexible beam link structure. The micro actuator consisted of a high bandwidth (3000 psi fluid with 1 in bore pistons) dual-acting hydraulic actuator capable of 45 g accelerations. In freespace motion, Sharon showed he could use the micro manipulator to compensate for positioning inaccuarcies of the flexible macro manipulator using the following control:

$$f = -G_1 x_3 - G_2 \dot{x}_3 \tag{2.17}$$

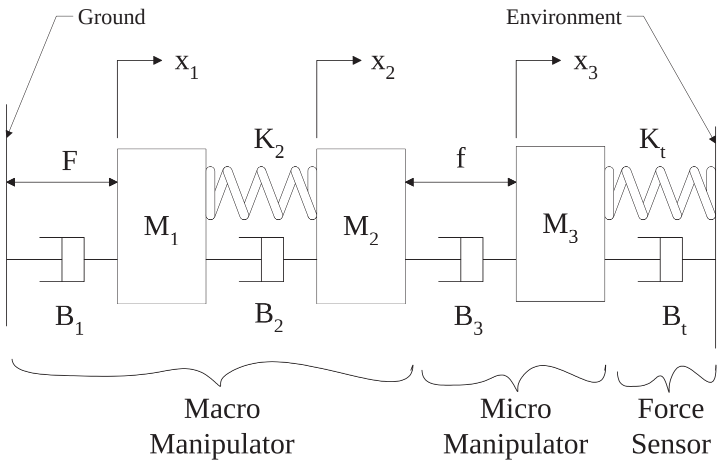

Figure 2-8: Sharon's macro-micro model. The macro manipulator is assumed flexible. K_t and B_t represent stiffness and damping of a force sensor mounted between the micro manipulator and ground during contact.

During position control, x_1 is assumed to be zero, that is exactly tracking the desired position/velocity. Also, it is assumed that the micro actuator has a limited positioning range, and is programmed to stop when it reaches the end of its workspace limit. The result is that the micro manipulator "jumps out ahead" of the macro manipulator and "locks on" to the desired endpoint position when the macro manipulator brings it within its workspace. Positioning bandwidth is thereby improved over the macro manipulator alone.

To study force control, a piezoelectric sensor was attached to ground and covered with a soft (15 lbs/in, 2600 N/m) covering. The manipulator pressed on this surface. The control was:

$$F = -G_1 x_1 - G_2 \dot{x}_1 \tag{2.18}$$

$$f = -G_3 F_t - G_4 \dot{x}_3 \tag{2.19}$$

The gains G_1 and G_2 were chosen to be impedance matched with the micro manipulator in order to remove energy from the system. The gains G_3 and G_4 were presumably tuned to give the best stable response. It was found that stable force control could be maintained with the caveat that the environmental stiffness be sufficiently soft. This was attributed to the use of a hydraulic micro manipulator whose output force could not be directly commanded, that is which acts like a flow source. Sharon suggests that a micro actuator which acts like an effort (force) source may be able to interact more successfully with a hard surface. He also suggests that if the micro actuator acts like an effort source and is therefore backdrivable, the macro-micro manipulator will be able to present a low impedance to the environment.

2.3.5 Force Measurements

As described above, there are certain cases where force measurements are beneficial. For example, in the case where large gear type reductions are necessary and substantial friction is therefore unavoidable, the use of force sensing might be appropriate help compensate for this friction. In the case of parallel-coupled micro-macro control a substantial increase in dynamic range is achieved using multiple actuators in conjunction with force sensing. However, several specific problems with force sensing should be discussed:

- Noise in the measurements. If measurements contain noise, either the system bandwidth must be maintained below the frequncy of the noise, or the noise must be filtered. Inputing noisy signals into a controller at best will introduce vibrations which the human operator can feel and will find annoying. At worse, noisy signals can excite unmodelled system dynamics and drive a system unstable. However, if force signals are filtered, another bandwidth limit is introduced which must be avoided. Stated otherwise, the filter will introduce lag into the controller which will limit the achievable gains and hence the controller's ability to reject disturbances.

- Drift in force sensor readings will make system "walk". For example, if the slave is commanded to output zero torques, but sensors on the slave drift slightly from zero, the slave motors will be commanded to move in order to zero these sensors. The master robot will track the positions of the slave robot. If the user prevents the master robot from moving, phantom forces will be felt corresponding the the drift forces in the sensor.

  This is similar to having uncompensated gravity terms in the controller. However, force sensor drift may occur in any direction and will likely be time varying since it is typically caused by changes in temperature. Tempurature changes are abundant in the surgical environment due to body fluids, saline for irrigation, and hot lights for endoscopy which will contribute to sensor drift, even if full bridges and thin sensor elements with high heat conductivity are used.

- Sensors introduce additional cost and complexity. Extra wiring and packaging is required as are A/D boards, bridge electronics and filtering circuitry.

- Force sensors typically consist of flexable element whose deformation (strain) is sensing and from which force is inferred. As a result, they tend to be delicate if they are sensitive and have a limited range based on allowable deflections before permanent deformations are introduced. Implementing force sensors in high degree of freedom systems is in itself a challenge.

2.4 Actuators

work on!

Actuator technology is another field unto itself, but a few comments are warranted concerning teleoperators in particular. In bilateral force reflecting systems, we typically want our actuators to behave as pure force/torque (effort) sources. As described above, much research has been focussed on this goal. Lorenz force actuators have the potential to behave this way, coverting input current into output effort. Since current may be controlled accurately at frequencies well above typical mechanical frequencies, this is a good choice.[1] A voice coil mounted on a frictionless flexure provides a high quality effort source. For example, Hi-Fi audio speakers using high quality audio amplifiers have low distortion in the tens of kHz range. There are obviously many other types of actuators such as hydraulics servoactuators which cannot be beaten for power to weight ratio, pneumatics, and more exotic types such as shape memory alloys. For small convenient effort sources, however, we maintain our focus on electric motors.

As opposed to voice coils, electric motors however must have substantial torque outputs and range of motion. Several schools of thought have arisen. One is to use direct drive motors. Typically iron core high inertia, large cogging, nlarge volume, slow speed, relatively high torque, e.g. Asada. Can be either brushed or brushless. Certain motors do not have cogging. Manipulators designed with current direct drive technology tend to be massive and therefore not well suited for a system which must interact with a delicate environment.

The other is to use not worry too much about the actuator and compensate with distal force sensing. Already discussed some of these options.

The other is to use fast, low inertia actuators, and high quality transmissions and speed reductions. This idea is in fact not new, coming from the original mechancal master-slave manipulators which required high quality transmissions to enable force

[1] For example, the off the shelf PWM current amplifiers (Copley Controls, model 303) which we use have a measured bandwidth of 400 Hz.

reflection. (Vertut and Coiffet, 1986) discusses the use of block-and-tackle cable transmissions used to reduce friction and intertia and to eliminate backlash on the French MA-23M bilateral force refelcting teleoperator.

Iron vs. Ironless: It is beneficial to have low rotor inertia when designing such systems because the effective output inertia contribution of the motor rotor is equal to the rotor inertia multiplied by the square of the reduction ratio. Therefore, with any substantial reduction, rotor inertia can dominate the total inertia in a hurry. Ironless core (basket or disk) motors then become a good choice for two reasons. First, they have low rotor inertia, and second, they have no cogging. This is because there are no pole pieces on the rotor to line up with permanent magnets which creates cogging. They have one important disadvantage: they have bad thermal properties. Because the rotor consists of wire encased in an epoxy resin, the rotor has small thermal inertia and must dissipate heat across an air gap to the motor stator (housing). Peak to continuous torque ratios are typically on the order of 10×. In Chapter 6 we show that water cooling can increase continuous torque limits by a factor of two.

Permanent magnet materials are critical when determining power and stall torque. The best magnets today are the Ne-Fe-Bo variety, with Sa-Co and Alnico being weaker. There are a number of manufacturers of basket motors (Maxon Motors, Micro-Mo, Escap) and disk motors (PMI), but Maxon Motors have typically been our favorite, largely because their "RE series" uses Ne-Fe-Bo magnets.

Brushed vs. Brushless: A significant amount of friction in a well designed system is contributed by motor brushes. For example PMI disk motors, while have low inertia and no cogging, have substantial brush friction. This is a function of the brush and commutator design. Brushless motors have the coils on the stator, and permanent magnets on the rotor. The advantage is there is no brush friction and no brush-life limitation, and thermal dissipation is improved because the coils dissipate heat to the house. In fact with water cooling, these motors can run at peak torque values continuously.[2] The disadvantage is the motor rotor is typically higher since they carry magnets, the commutation electronics can be expensive, and the commutation electronics themselves can contribute cogging even if the rotors intrinsically have none, (Levin, 1990).

2.5 Cable Design

work on!

[2]Underwater manipulators such as those used at Woods Hole Oceanographic Institute use the cold seawater as a motor heat sink and are designed to run at peak torques continuously.

So how do we design high quality transmissions? In my experience, the best method for implementing a low friction, backlash free transmissions in a high degree of freedom manipulator with severe space constraints is to use mechanical cabled transmisions, (Flatau, 1973), (J.K. Salisbury, 1982), (Vertut and Coiffet, 1986), (Townsend, 1988), (DiPietro, 1988), (Salisbury et al., 1989), (Salisbury et al., 1990), (Schempf, 1990), (Massie and Salisbury, 1994).

A number of different materials can be used. Most commonly used is stainless steel aircraft cable (SAVA Industries, Baird Industries). Critical design factors are:

construction. minimum fiber size. coatings. lubricants. pulley diameter. pulley groove shape. reverse bending.

These factors contribute to: strength. fatigue life. abrasion resistance. corrosion resistance. friction: due to plastic deformation, fiber/fiber rubbing, cable/pulley rubbing.

other materials:

tungsten - higher modulus, better wear resistance. spectra fiber (now sold commerically as Spiderwire fishing line.) vectran fiber. polyethelene fibers.

Many types of speed reductions possible:

block-and-tackle. rotarty-to-linear wire drive. rotary to rotary, limited angle reduction. frictional connection. terminated connection.

Idlers:

idlers are preferably pulleys instead of runners. pulley should not be hard (for abrasion). Hard anodize hurts. delrin is low friction but can wear due to lack of toughness. nylon is softer, but tougher and better for cable wear. other materials may be effective such as teflon filled delrin.

2.6 Comments on Human Perception

In Section 2.2.1, we discussed the tradeoff between stiffness and inertia in the teleoperator. In order to make this tradeoff as a designer, it is helpful to understand how humans perceive inertia and stiffness. Human perception and haptic perception in particular are broad fields of research, see for example (Boff et al., 1986). Here we intend only to make a few general comments.

- Humans cannot distinguish feel finite stiffnesses above roughly 25,000N/m between infitite stiffnesses, according to (Tan et al., 1994). These experiments were performed by placing a flexable aluminum bar in the vise of a milling machine and pushing on the bar (with eyes closed) at distances increasingly close to the vise, which is effectively completely rigid. This was done with fingers, the palm of the hand and the forearm with similar results. Above a stiffness of 25,000N/m, the bar was indistinguishable from the vise itself, despite deflections of as much as several cm.

- Humans are very sensitive to vibrations. During the same experiments by (Tan et al., 1993), tapping on the bar and sensing the resulting vibrations allowed the subjects to move within several cm of the vise and discern the difference in stiffness with much greater resolution. (Bolanowski et al., 1988) showed that humans can detect nearly as small as 0.1 μm amplitude vibrations of at 300 Hz on the thenar eminence (the group of muscles at the base of the thumb between the base of the thumb and the wrist). (Sherrick and Cholewiak, 1986) gives a value of between 0.2 μm and 0.5 μm at 200 Hz to 400 Hz again for stimulation of the thenar eminence. While sensitivity decreases at lower or higher frequencies, amplitudes of 5 μm to 20 μm can still be detected at frequencies as low as 30 Hz.

- Humans are sensitive to changes in stimulus, but are relatively insensitive to constant stimulus. To some extent, we are "AC coupled". As a result, the notion of isotropy is important in teleoperator design in order to provide transparency. Friction and inertia present disturbance forces to the human user of a teleoperator. However, if these disturbances are not time varying, are distributed evenly in space, and are the same in all directions, hence isotropic, then humans will be much less sensitive to them than otherwise.

  Also, a system with non-isotropic friction and inertia will have preferred directions of motions. That is, motions in certain directions will be easier than in others. This is distracting and confusing to a user especially when making fine motions.

- Gravitational forces, though constant, cause fatigue. A system can have a considerable amount of inertia which, if isotropic, may not be bothersome to a user. But if the user must carry the weight of the system, they will quickly become fatigued and consequently annoyed. This comment is based on personal experience co-designing the SaFire force-reflecting hand interface for Exos, Inc.[3] A constant weight of as little as 2 lbscarried on the user's forearm caused considerable fatigue. The device was eventually counterbalanced with a table mounted boom.

[3]Exos Inc. of Woburn, MA has since been purchased by Microsoft, Inc., Redmond, WA.

2.7 Manipulator and Telemanipulator Hardware

There are several excellent books on telerobotics and human-in-the-loop computer control of mechanisms such as (Sheridan, 1992) and (Vertut and Coiffet, 1986). There are scores of different manipulators and books on them. Here we mention a few systems which we find interesting, in particular to give a little historical perspective on cable driven designs.

The field of telerobotics is by now not new, having its beginning in purely mechanical master/slave manipulators used in radioactive hot-cells. (For a more extensive history, see (Vertut and Coiffet, 1986)). The first mechanical master-slave system, the M1, was developed by Raymond Goertz at Argonne National Laboratory in the mid 1948. The M1 and roughly a dozen later models used a series of mechanical linkages and steel cables to connect a master manipulator to a kinematically identical slave manipulator on the other side of a lead-glass barier. (Goertz, 1954) briefly describes the Model 8. Later, the advent of servomechanisms allowed the mechanical linkages to be replaced by servomotors, though the kinematically identical nature of the manipulators remained, (Goertz and Thompson, 1954). These manipulators were force reflecting.

It is interesting to note that the prior to the development of mechanical teleoperators, (and after the dangers of radiation were discovered), nuclear laboratories used *remote handling tongs* which passed through a spherica joint in a lead wall to handle radioactive materials. A mirror arrangement was used to view samples. These tongs were nearly identical in design to modern minimally invasive (laparascopic) graspers and needle drivers, /citeVertut:1986: states that: “There are clearly a number of difficulties that arise from the inversion of the movements of the gripper in relation to those of the handle, and from working with the mirror image of the scene. The need for a method of manipulation, which involved little training and provided complete dexterity foro handling the first radioadtive metallic or chemical samples in laboratory experiments, was clear.” These motivations completely parallel those for teleoperation in minimally invasive surgery.

In the 60’s and 70’s, Carl Flatau, originally of Brookhaven National Laboratory, championed cable drive manipulators for teleoperation with such designs as that proposed for the MIT A.I. lab mini-robot project (Flatau, 1973), the MA-22-A Arm (Flatau et al., 1972), and the Telemac, designed to perform nuclear facility maintenance.[4] (Vertut and Coiffet, 1986) also describes another interesting arm developed at CEA in France, the MA-23M. This is a descendent of the MA-22-A which

[4]By personal communication (phone conversation), Carl Flatau, Director, The Bartholemew Co., Telerobotic Division, Westbury, N.Y., 1991.

uses cable and tape drives exclusively as speed reductions, that is no gearing in the shoulder, in order to make the system more backdrivable and to eliminate backlash. It uses existing motor weight to counterbalance the weight of the arm.

The Salisbury hand and the Utah/MIT hand are both examples of cable/tendon driven manipulators, (J.K. Salisbury, 1982), (Narasimhan, 1988). The Salsbury hand uses three fingers with four degrees of freedom each. The fingers are actuated by cables (four for each finger in an N+1 configuration) which run through telfon-lined flexible metal conduits to a motor package which can be placed remotely, for example on the forearm of a PUMA arm for example. The Utah/MIT hand has four four degree of freedom fingers actuated using polyethylene tendons (originally these were Kevlar) strung through a tendon remotizer to a remote pneumatic actuator package. The remotizer is essentally a seperate arm consisting of links and pulley over which the tendons are routed to maintain a constant cable length as the hand is moved. Both hands incorporate tendon tension sensors to better modulate output forces.

The WAM (Whole Arm Manipulator) is a four degree of freedom arm developed at the MIT A.I. Lab which is again entirely cable driven, , (Townsend, 1988)(Salisbury et al., 1989). This arm is also backdrivable, has no backlash in the joints and can perform very fast motions without disturbances which would normally accompany a gear drivetrain.

Another cable driven arm is the WHOI (Woods Hole Oceanographic Institution)/MIT arm developed for the ARGO/JASON project, (DiPietro, 1988). For an extensive treatment of robotic transmissions, see (Schempf, 1990).

2.8 Haptic Interfaces

Haptic Interfaces are used either as the master side of a master/slave telerobot, or as an interface to a virtual environment where the sense of touch or force is imparted to the user. Again, there are many examples of hardware and we mention only a few. Note our emphasis is on imparting forces to the user as opposed to tactile senses using tactile displays and on higher degree of freedom system as opposed to force reflecting joysticks, and on cable driven devices.

Salisbury developed a cable driven six degree of freedom hand controller at JPL, . This system used revolute joints and a single sliding joint in a gravitationally counterbalanced configuration. A descripion of the device is given in (Bejczy and Jr., 1983), and performance analyses were done by (Hannaford et al., 1991). Unfortunately, the slave used in these experiments was PUMA arm mounted with a wrist force/torque sensor.

In 1992 and 1993 EXOS, Inc, led by Dr. Beth Marcus, developed two force reflecting exoskeletal devices. The SAFiRE™ is a 7 degree of freedom (2 DOF index, 3 DOF thumb, 2 DOF wrist) hand exoskeleton designed to work with "glove-box" simulations of shuttle experiments in 0 g. The Force ArmMaster™ is a four degree of freedom (3 dof shoulder, 1 dof elbow), arm exoskeleton. Both systems use combinations of planetary gear reductions and cable reductions to achieve the necessary speed reduction.

In 1993, Thomas Massie and Ken Salisbury at the MIT A.I. Lab developed the Phantom haptic interface, (Massie and Salisbury, 1994). This interface is essentially a three degrees of freedom powered arm which gives force, but not torque, feedback to a user. A passive three degree of freedom quarter-gimbal mounted at the the end of the arm allows the user's fingertip (or a stylus) to attach to the end of the arm without constraining rotations. Several nice features include gravitional counterbalancing, low friction cable drive speed reductions, and relatively isotropic friction and inertia through much of its workspace.

2.9 Teleoperators for Surgery

Teleoperators for surgery are a subset of the manipulators, telerobots and haptic interfaces. There are two areas which have received focus within the past three years, largely due to the efforts of Col. Richard Satava, M.D., formerly a project leader at DARPA. The first, championed by Col. Satava is the idea of battlefield surgery where surgeons well back from the front lines perform surgery using telerobots installed in armored vehicles on the front lines. These systems are for performing open surgery in a remote location. The second area which is gaining ground in the commercial sector, and which is the focus of this thesis, is that of minimally invasive surgery.

SRI's open telesurgical system, was at the forefront of this movement (Hill et al., 1994). This system uses two five degree of freedom slaves, and two kinematically identical masters mounted within a surgeon's console. The arms use spherical kinematics and a gripper (pitch, yaw, in/out, roll, and grip).The console uses a video monitor which is mounted so that a mirror reflects the image to a surgeon wearing polarized 3-D glasses. The monitor uses an LED screen to polarize the images from two CCD cameras mounted at the operating site alternately in the north-south and east-west directions to give the user a stereo image. The surgeon places their hands beneath the mirror such that, if everthing is alingned correctly, the instruments which they hold (attached to the masters) coincide visually with the slave instruments. The most striking thing about this system is that effect of the illusion created in this way is extremely effective. The system has some degree of force reflection. The author found that it was difficult to distinguish the difference in stiffness between, for example, the fleshy part of the hand and hard knuckle being pressed on by the slave.

At JPL, a microdexterity robot was developed, (Schenker and Charles, 1995). This robot appears to have a needle at the output, as opposed to a gripper which would be need to actually perform surgical tasks. It uses gear reductions and cables to drive its joints. The wrist used is a variant of the Rosheim wrist (Rosheim, 1989). The focus here is microsurgery, as opposed to remote or minimally invasive surgery.

In the corporate sector, substantial efforts are being made to commercialize telerobotics for minimally invasive surgery. Perhaps the two most important companies in this area are Intuitive Surgical, Inc., Mountain View, CA, and and Computer Motion, Inc., Goleta, CA. Intuitive Surgical is developing a two arm master/slave system for MIS named DaVinci, and Computer Motion is developing an MIS system called ZUES. Computer Motion has been selling for several years a robotic endoscope holder known as AESOP. (Mehta, 1997)

2.10 Summary

The basic teleoperator control discussed at the beginning of this chapter can be guaranteed to be stable (it is passive), but suffers in that the inertia of both the slave and master are felt by the user. For a system which must perform surgery, we suspect this will simply be too high to achieve reasonable force feedback. Therefore, some method of controlling manipulator endpoint forces is needed and feeding these back to the master is required. We will study how this can be done in Chapter 3. In particular, we will revisit the idea of macro-micro control using a considerably different experimental system than used by (Sharon, 1988) which more accurately reflects our goals and design techniques, in addition to the fact that it is a master/slave system as opposed to a single manipulator. We show that using a two degree of freedom macro-micro slave manipulator coupled to a one degree of freedom master we can achieve well-behaved force scaled teleoperation with a force scale factor of 50:1 with the use of a force sensor.

While there have been many teleoperators and haptic interfaces designed, there are no systems which allow teleoperated minimally surgery with force reflection and with manual dexterity comparable to that of open surgery. We hope that the systems presented in this thesis will help to fill that gap and lead to a new generation of surgical instruments: teleoperators for minimally invasive surgery.

Chapter 3

Macro-Micro Actuation

In this chapter we investigate several methods to control a master-slave system where a macro-micro manipulator is used as the slave. We define a macro-micro manipulator as one consisting of a lightweight distal manipulator mounted on a heavier proximal manipulator.

We present data from five different controllers using a three degree of freedom testbed to demonstrate our approach. Of the controllers we tested, we found a Jacobian Inverse controller to provide stable, crisp bilateral force reflection with 50:1 force scaling on a testbed with a one degree of freedom master and two degree of freedom "macro-micro" slave. The goal is to develop an approach which can be extended to our later 7 and 8 degree of freedom teleoperator designs, the Silver Falcon and Black Falcon.

3.1 Introduction

If we look at the basic force-reflecting teleoperator in Chapter 2, we can see that when moving the teleoperator through free space the human operator will feel the inertia of both the master and the slave. Therefore, to make the system feel as light as possible it seems reasonable to design the master and slave manipulators to be as light as possible. Of course, we are limited because actuators have limited power to weight ratios and materials have limited strength and stiffness.

The idea is based on the supposition that the slave can be designed to have a "sensitive" end effector (wrist and fingers) which is lightweight and low in friction. Then we ask: if this wrist is mounted on the end of a larger manipulator, with consequently larger inertia, would it be possible to make visible to the master only the inertia of the smaller, lighter end effector? In this chapter, we compare several methods of control as part of this approach.

We demonstrate the idea using a testbed consisting of a one degree of freedom master and a two degree of freedom slave described herein. The master is essentially an actuated rotary turntable with a knob which the user can grasp. The slave has two actuators, a macro actuator base and a micro actuator mounted upon it whose endpoint inertia is 200 times lower than that of the macro actuator. We demonstrate high quality, force-reflecting teleoperation with force scaling of 50:1, without the use of explicit force sensing. The control effectively (a) hides most of the inertia of the slave manipulator from the user who feels only the inertia of the master and that of the slave micro actuator end effector, and (b) therefore makes the slave respond more readily to forces from the environment.

An inertesting question which arises is whether we wish to reduce the inertia of the master as well. After all, the user feels both the inertia of the master and the slave, so if we wish to reduce slave inertia, why not reduce master inertia as well? The reason has to do with force scaling, which breaks the inherent symmetry of the system. If we scale forces such that master forces are magnified with respect to slave forces, as we will in this chapter, then the master must be able to achieve a proportionately higher servo stiffness than the slave. Reducing the inertia of the master reduces the the servo stiffness which the master can achieve, (see Chapter 2). In this case, we would like the master to have an inertia larger than the slave in direct proportion to the force scale factor.

3.2 Prototype Hardware

These ideas were studied using the testbed shown in Figure 3-1. A schematic drawing is shown in Figure 3-2 where system variables are defined.

The slave has two degrees of freedom, a macro and a micro freedom. The master has one degree of freedom. All three axes are driven by brushed d.c. servomotors (Maxon Motors RE025-055-035EAA200A). In our discussion of the system, we scale all joint forces and positions by link lengths implicity in order to avoid carrying these values through the calculations. In order to keep with general notation for joint forces and positions, these are labelled τ_i and q_i respectively, and have units of newtons and meters. Inertias are also measured at the endpoint of each joint and have units of kilograms.

The first joint position of the slave is labelled q_1 and the output force for this joint (force at the tip of the link) is τ_1. This first axis is driven by a low friction,

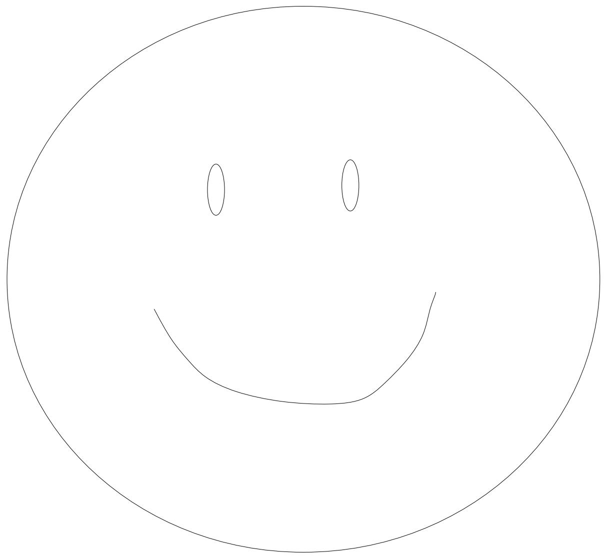

Figure 3-1: Photo of the macro-micro testbed.

one stage cable reduction with a ratio of 13.87:1. The axis one encoder is a Hewlett-Packard optical encoder with 2000 counts per revolution after quadrature. The output resolution is therefore 27,740 counts per revolution. At a link length of $l_1 = .0635$ m (2.5 in), this gives an endpoint resolution of 1.44×10^{-5} m (5.66×10^{-4} in).

The second joint is mounted to the first joint such that its axis is orthogonal to and intersecting with the first. The second joint position is labelled q_2, and the output force of this second joint is labelled τ_2. Mounted to the shaft of the joint 2 motor is a "T" shaped output link[1]. This second joint is direct drive and uses a Canon laser encoder (TR-36) with 14,400 counts per revolution after quadrature. At a link length of $l_2 = .025$ m (1 in), this gives an endpoint resolution of 1.11×10^{-5} m (4.36×10^{-4} in).

The master is a single rotary joint whose position is labelled q_3. The force for this joint is τ_3. The master is driven by a single stage cable reduction with a ratio of 10.67:1. The encoder on this axis is a Hewlett-Packard optical encoder with 2000 counts per revolution after quadrature, giving a total resolution of 21,340 counts per revolution. At a link length (the point where the user holds the master) of $l_3 = .044$ m (1.75 in), this gives an endpoint resolution of 1.29×10^{-5} m (5.1×10^{-4} in).

The inertia for joint 1, the macro axis, is 1.16 kg. The inertia of joint 2, the micro,

[1]The reason for this "T" shape is to dynamically balance the link as a safety measure. This prevents bending of the motor shaft at high shaft velocities.

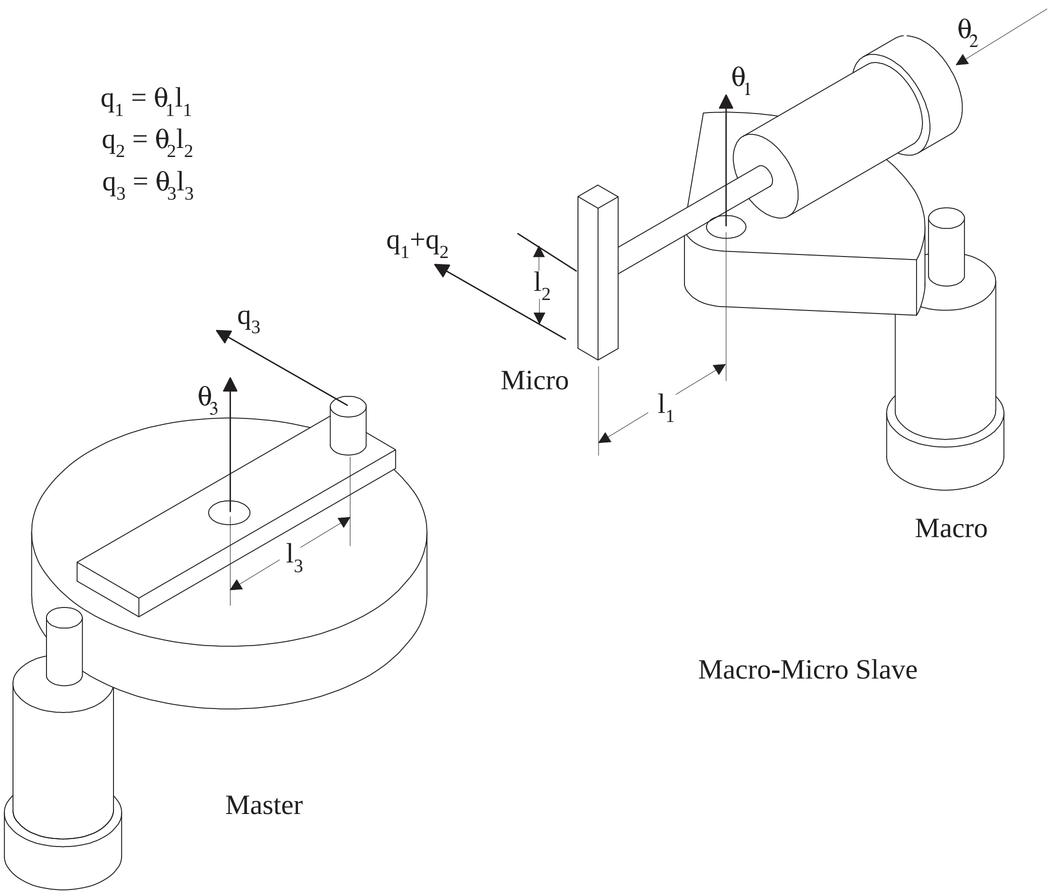

Figure 3-2: The slave consists of a single motor with a "T" shaped output shaft resting on a base turntable driven with a cable reduction. The master is a single turntable driven with a cable reduction.

is .006 kg, and the inertia for joint 3, the master, is 1.53 kg. These values were found by simulating a mass-spring-damper system with the same spring and damping values as programmed into the real system and adjusting the mass until the simulated and experimental responses coincided. The nominal controlled damping value was zero. Some damping was added to the simulation to compensate for friction in the system.

The friction in each axis was measured using a digital force sensor (Mark 10 Model BG2). The friction in joint 1, the macro, is approximatly 0.47 N, the friction in joint 2, the micro, is 0.02 N, and the friction in joint 3, the master, is 0.54 N.

Add paragraph on the electronics

3.3 Individual Joint Performance

To give an idea of the performance of each axis acting individually, we looked at individual position control response for each joint. Each axis was controlled with a simple position-derviative (P.D.) controller:

$$\tau_i = -K_i q_i - B_i \dot{q}_i \tag{3.1}$$

The P.D. gains we use for these responses are the same gains (in some cases they are slightly different) used for controllers presented later in this chapter to achieve 50:1 force scaling. In order to achieve this high force scaling, the stiffness gains for the macro and master were tuned to be as high as possible, given limitations in the stable damping which we could achieve. Then the micro stiffness and damping gains were tuned to be 50 times less. The q_1 macro gains were 7000 N/m and 55 Ns/m, the q_2 micro gains were 160 N/m and 1.3 Ns/m, and the q_3 master gains were 8000 N/m and 65 Ns/m. As expected, 8000/160 = 50. The servo rate was approximately 6000 Hz for all data presented in this chapter.

describe friction compensation algorithm

Step responses for each axis are shown in Figures 3-3, 3-4, and 3-5. Note that the master and macro responses are underdamped, while the micro response is nearly critically damped. This is expected given the gains which were selected. If we ignore for the moment existing natural friction in the system, the damping ratios ζ_i for each axis are given by:

$$\zeta_1 = \frac{B_1}{2\sqrt{K_1 m_1}} = \frac{55 \text{ Ns/m}}{2\sqrt{7000 \text{ N/m} 1.16 \text{ kg}}} = 0.31 \tag{3.2a}$$

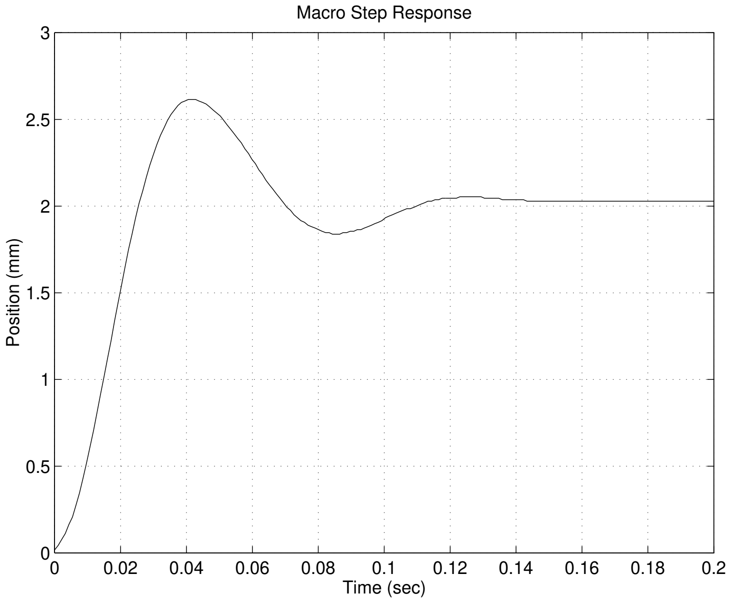

Figure 3-3: Step response for the q_1 macro actuator.

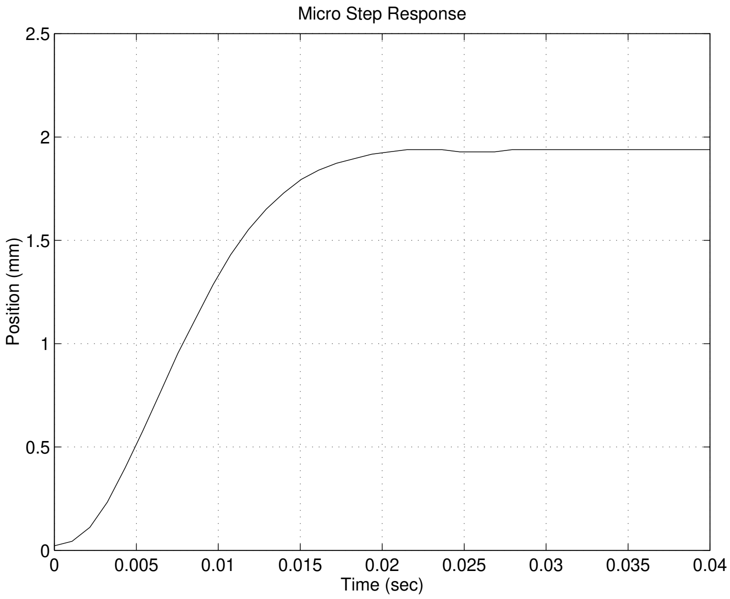

Figure 3-4: Step response for the q_2 micro actuator.

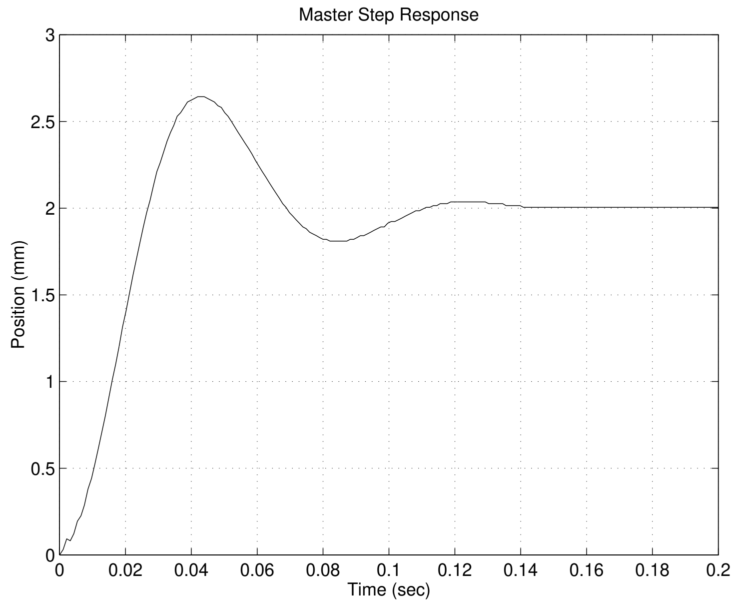

Figure 3-5: Step response for the q_3 master.

$$\zeta_2 = \frac{B_2}{2\sqrt{K_2 m_2}} = \frac{65 \text{ Ns/m}}{2\sqrt{8000 \text{ N/m} 1.53 \text{ kg}}} = 0.29 \tag{3.2b}$$

$$\zeta_3 = \frac{B_3}{2\sqrt{K_3 m_3}} = \frac{1.3 \text{ Ns/m}}{2\sqrt{160 \text{ N/m} .006 \text{ kg}}} = 0.66 \tag{3.2c}$$

In fact, looking at the plots, the damping ratios appear higher which we would expect given that some naturally occuring friction exists in the joints which we only partially compensate for.

These “classic” second order responses show that a cable reduction drive with very little free length of cable (cable which is not wrapped around a drum) can introduce very little additional dynamics even with 10-13 times reduction. This is typically not the case with geared reductions for example. If you look carefully, you can see a small bump at beginning of the master response. This is due to a slight flexibility in the master cable transmission. A similar slight ripple occurs in the other master response plots. Other than that, transmission dynamics are not visible in the plots.

While the macro and micro axes differ by a factor of roughly 200, the positioning bandwidth differs only by a factor of roughly 5. Our primary goal in designing a controller is to take advantage of the large difference in macro and micro inertias, not to compensate for any dramatic difference in their servo bandwidth. Each axis has been designed to be a high quality system with low friction and zero backlash.

3.4 Control Methods

Below we describe 5 different methods for controlling our macro-micro system. In the process, we find out what the relevant benefits and pitfalls of such a system are and demonstrate stable, well-behaved master-slave teleoperation with 50:1 force scaling over a reasonable range of motion.

2 basic tests were done for each controller, step response and contact response tests. These tests show the speed of response and qualitativey show stability at two extremes of the spectrum, during free space motions and while contacting rigid objects.:

- Step response tests. In these tests, the initial condition for the master and slave are stationary and positioned 2 mm apart. The micro joint q_2 is stationary and positioned at approximately zero. The command is a step in endpoint position such that the desired endpoint positions are indentical. The motions of the master q_3, macro q_1 and slave endpoint $q_1 + q_2$ were plotted.
- Contact response tests. In these tests, I moved the master such that the slave moved towards and then contacted a rigid aluminum block. The motions of the master q_3, macro q_1 and slave endpoint $q_1 + q_2$ were plotted.

3.4.1 Basic Teleoperator

This is the gold standard by which we compare the other controllers. Here we apply the basic teleoperator control described in Chapter 2 to the master and micro actuator alone. The macro actuator is locked in place with clamps. The controller ties the master and micro together with a spring and damper. We label the endpoint forces for the master and slave F_m and F_s, and the cartesian stiffness and damping gains as K_m, B_m, K_s, B_s:

$$F_m = -K_m(q_3 - q_2) - B_m(\dot{q}_3 - \dot{q}_2) \tag{3.3a}$$
$$F_s = K_s(q_3 - q_2) + B_s(\dot{q}_3 - \dot{q}_2) \tag{3.3b}$$

In order to achieve 50:1 force scaling, we set K_m to be 8000 N/m, which is the highest we can reasonaby achieve and set $K_s = K_m/50 = 160$ N/m. The damping gains were $B_m = 65$ and $B_s = 1.3$. Because the master and slave have only one degree of freedom each, the joint forces are $\tau_2 = F_s$ and $\tau_3 = F_m$. We should note that this master slave connection is passive in the sense discussed in Chapter 2 as long as the master and

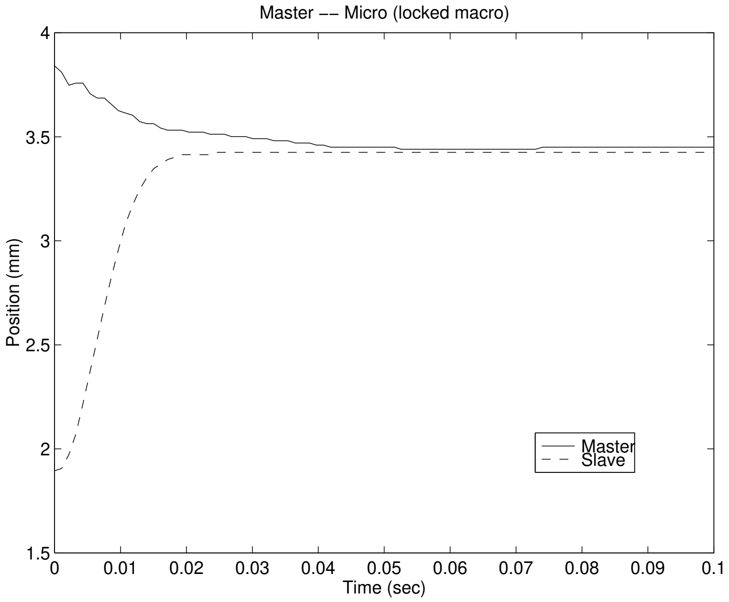

Figure 3-6: Step response for the master and micro axes slaved together using basic teleoperator control.

slave manipulators do not touch each other so that the only connection is through the controller.

The 2 mm step response is shown in Figure 3-6. Because the micro freedom, labelled "Slave" in the figure is so much lighter than the macro freedom, it moves considerably more than the master as they move together to achieve the same end-point position. Figure 3-7 shows the contact plot for this system. The master is moved by hand and the slave quickly follows. The slave makes contact with an aluminum block and stops abruptly and the contact is well behaved and stable. The master overshoots slightly due to the finite stiffness connection between the master and slave. The force created by the resulting position error however quickly stops the master and its position settles to the slave position value as pressure is released by the user. The commanded output forces which the master applies to the user are 50 times that which the slave applies to the aluminum block. The actual output forces differ by the small amount of friction in the systems and by the forces required to decelerate the very light aluminum micro output link.

The actual feeling which the user experiences is fairly dramatic. Because the position has not been scaled between the master and slave, the effective stiffness of objects in the environment is multiplied by 50 when felt through the master. Contact with the aluminum block is felt sharply and clearly at the master. Another excellent

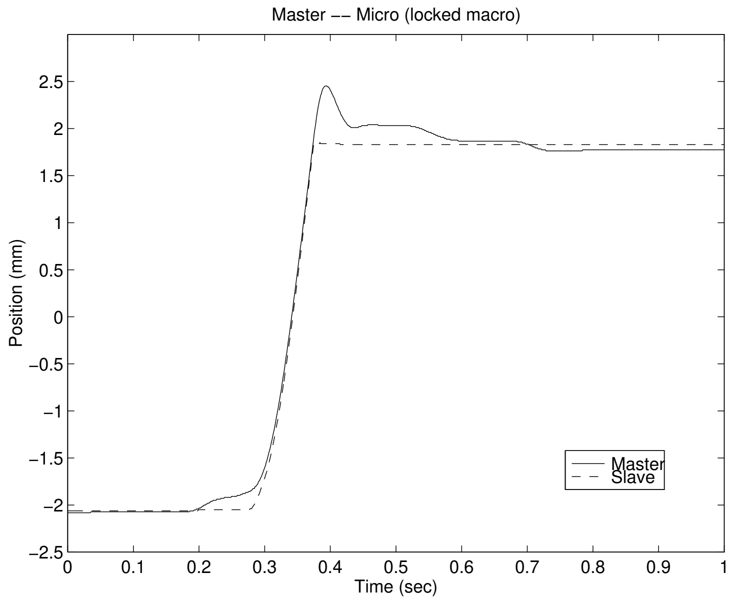

Figure 3-7: Contact response for the master and micro axes slaved together using basic teleoperator control.

example is poking the slave using soft foam. It is easy to shove the master around (and the user holding on to it) with a piece of very soft foam or kleenex tissue. Trying to push a standard eraser across the table with the slave from the master side of the connection feels like pushing a desktop telephone.

The problem with this system is that the range of motion of the micro actuator is limited in this case to only a few centimeters. The price of having a very light, low friction slave is that it must also be small. As a result, motions of the master are limited to a small portion of it's workspace. The next four controllers represent different ways to use the macro actuator to increase the range of motion of the entire slave manipulator.

3.4.2 Jacobian Transpose Controller

This controller is passive in the same sense as the previous controller and is probably the most straightforward method of cartesian control of a multiple degree of freedom slave manipulator. In this case, a cartesian error is calculated between the master and slave endpoints and is multiplied by a cartesian P.D. to produce desired endpoint forces. Also, because our slave is one degree of freedom, we set the desired slave endpoint orientation is zero and apply an additional P.D. to maintain this orientation.

These endpoint forces will then be mapped to the joint torques via the transposed jacobians for each manipulator. The endpoint forces are given by:

$$\begin{aligned} F_m &= -K_m(q_3 - q_s) - B_m(\dot{q}_3 - \dot{q}_s) && (3.4a) \\ F_s &= K_s(q_3 - q_s) + B_s(\dot{q}_3 - \dot{q}_s) && (3.4b) \\ F_{q2} &= -K_{orient} q_2 - B_{orient} \dot{q}_2 && (3.4c) \end{aligned}$$

where:

$$q_s = q_1 + q_2 \tag{3.5}$$

Then our Jacobian is given by:

$$\begin{pmatrix} \dot{x}_s \\ \dot{q}_2 \end{pmatrix} c = \begin{pmatrix} 1 & 1 \\ 0 & 1 \end{pmatrix} \begin{pmatrix} \dot{q}_1 \\ \dot{q}_2 \end{pmatrix} = J\dot{\mathbf{q}} \tag{3.6}$$

The joint torques are found using the transposed Jacobian:

$$\begin{aligned} \tau_3 &= F_m && (3.7a) \\ \begin{pmatrix} \tau_1 \\ \tau_2 \end{pmatrix} &= \begin{pmatrix} 1 & 0 \\ 1 & 1 \end{pmatrix} \begin{pmatrix} F_s \\ F_{q2} \end{pmatrix} = J^T \begin{pmatrix} F_s \\ F_{q2} \end{pmatrix} && (3.7b) \end{aligned}$$

We find controller viewed at the joint level is:

$$\begin{aligned} \tau_1 &= K_s(q_3 - q_1 - q_2) + B_s(\dot{q}_3 - \dot{q}_1 - \dot{q}_2) && (3.8a) \\ \tau_2 &= K_s(q_3 - q_1 - q_2) + B_s(\dot{q}_3 - \dot{q}_1 - \dot{q}_2) - K_{orient}\dot{q}_2 - B_{orient}\dot{q}_2 && (3.8b) \\ \tau_3 &= -K_m(q_3 - q_1 - q_2) - B_m(\dot{q}_3 - \dot{q}_1 - \dot{q}_2) && (3.8c) \end{aligned}$$

The individual joint gains used were:

$$\begin{array}{ll} K_s = 160 \text{ N/m} & B_s = 1.3 \text{ Ns/m} \\ K_m = 8000 \text{ N/m} & B_m = 65 \text{ Ns/m} \\ K_{orient} = 50 \text{ N/m} & B_{orient} = 0.5 \text{ Ns/m} \end{array}$$

The problem with this controller is that the inertia of the macro q_1 (1.15 kg) is felt at the master q_3 multiplied by the force scale factor of 50. In addition, the user feels the inertia of the the master or $50 \times 1.16 + 1.54 = 59.7$ kg. Figure 3-8 shows the 2 mm step response for the system with the Jacobian Transpose contoller. Because the apparent macro inertia is so large, it barely moves and all compensation is done by the master and micro axes. The endpoints come together and are also pulled towards the macro position. The final micro deflection is roughly .5 mm to

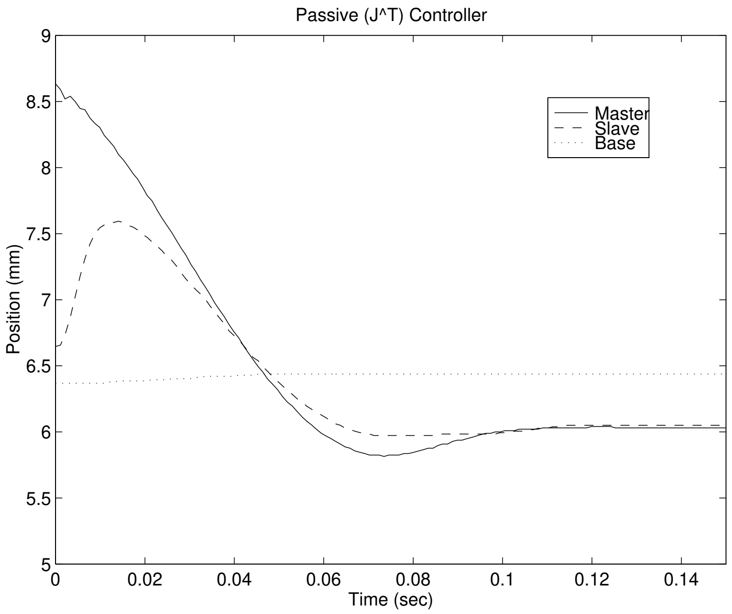

Figure 3-8: Step response for the master and slave using the Jacobian Transpose control.

compensate for the immovable macro axis.

When trying to move the system by pushing on the master, the macro axis is again immovable, see Figure 3-9 The master motor reaches its torque limit after about 9 mm deflection and contact with the aluminum block is never made. At an 8000 N/m master stiffness, this means about 72 N of force was applied and the macro axis had yet to move.

3.4.3 Jacobian Inverse Controller

In this section, we describe a controller which uses the micro actuator to hide the inertia of the macro actuator. We will show in Section 3.4.3.1 that this is in fact standard Jacobian Inverse manipulator control, which reduces to the controller presented below when applied to our system.

The controller is given as follows. First we simply command the master to follow the position of the tip of the slave manipulator:

$$\tau_3 = -K_3(q_3 - x_s) - B_3(\dot{q}_3 - \dot{x}_s) \tag{3.9}$$

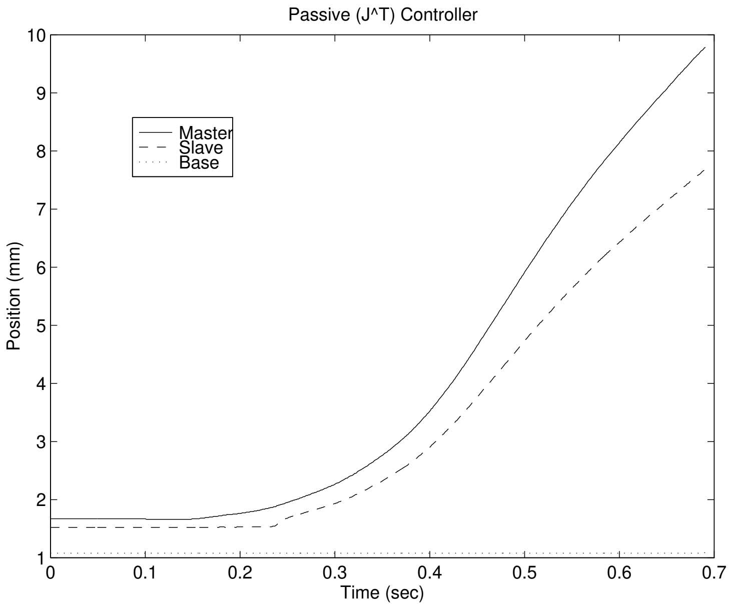

Figure 3-9: Contact response for the master and slave using the Jacobian Transpose control. Contact is never actually made here because the base is essentially immovabe and the master hits a torque limit in trying to move it.

where

$$x_s = q_1 + q_2 \tag{3.10}$$

Next we command the macro to follow the position of the master without regards to the micro position:

$$\tau_1 = -K_1(q_1 - q_3) - B_1(\dot{q}_1 - \dot{q}_3) \tag{3.11}$$

Finally, we command the micro actuator to remain at zero:

$$\tau_2 = -K_2 q_2 - B_2 \dot{q}_2 \tag{3.12}$$

The gains are then tuned to provide as stiff a master and macro as possible and then the micro gains are tuned such that the total endpoint stiffness of the slave is 50 times less than that of the master in order to provide 50× scaled force reflection. The gains which provide this are:

$$\begin{array}{ll} K_1 = 7000 \text{ N/m} & B_1 = 55 \text{ Ns/m} \\ K_2 = 163.74 \text{ N/m} & B_2 = 1.331 \text{ Ns/m} \\ K_3 = 8000 \text{ N/m} & B_3 = 65 \text{ Ns/m} \end{array}$$

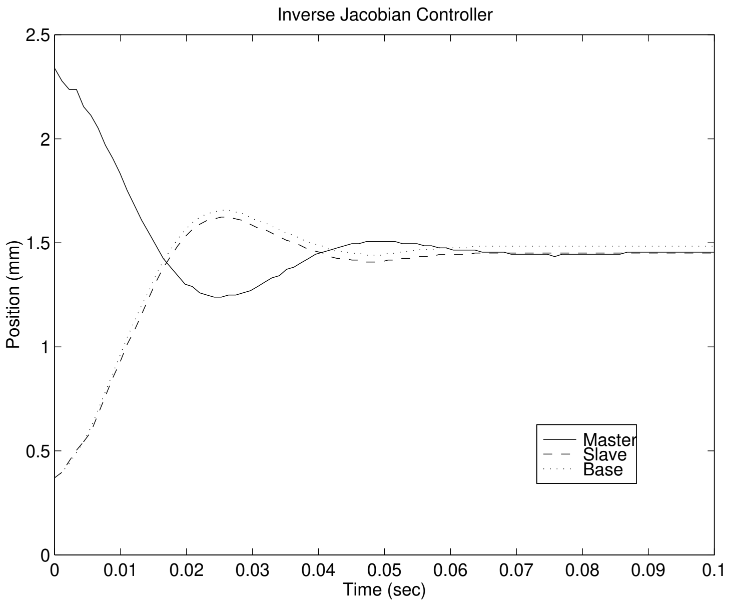

Figure 3-10: Step response for the master and slave using the Jacobian Inverse control.

The macro and micro stiffnesses form springs in series, so that:

$$(163.74 \times 7000)/(7000 + 163.74) = 160 \text{ N/m}$$

It is important to note that the micro axis is decoupled from the macro axis. Regardless of the position of the master or macro axes, the micro axis simply tries to remain at its zero position.

Figure 3-10 shows the 2 mm step response for this controller. The master and macro respond to each other and come together in straightforward second order responses. Since the inertia of these axes are similar they essentially mirror each others motions. The micro axis barely moves during the motion. The response appears well behaved and stable. Figure 3-11 shows a contact response plot for the Jacobian Inverse controller. Initially the master and slave are moving together towards an aluminum block. The slave hits the block and its tip position comes immediately to rest. The master actuator overshoots the slave tip position due to its finite servo stiffness, but quickly comes to rest. The macro (base) comes to rest at the position of the master. The roughly .25 mm offset between the master and slave represents a constant force being applied by the slave against the aluminum block and 50 times that force being applied to the user. The difference in the curves labelled Slave and Base (Macro) represent the relative motion between the micro and macro motions. While the micro stays in contact with the block, it deflects relative to the macro

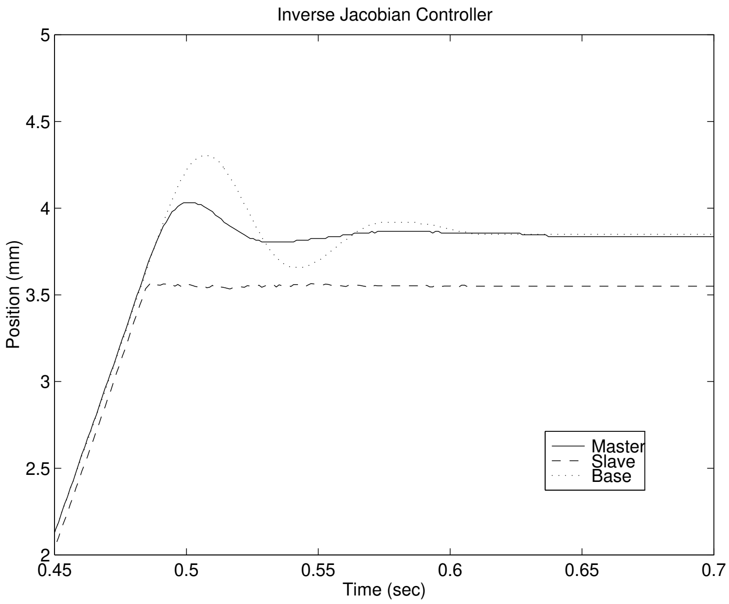

Figure 3-11: Step response for the master and slave using the Jacobian Inverse control.

actuator.

This controller is well-behaved during contact and provides crisp feeling scaled force reflection. During freespace motions and during contact, the feel is very similar to that of the basic teleoperator of Section 3.4.1. It has the important advantage however that the range of motion is equal to that of the macro actuator. Because the inertia of the macro actuator is hidden, its range of motion can be arbitrarily increased by making it larger as long as care is taken to increase motor sizes in order to maintain good positioning bandwidth.

analysis which shows that inertia is reduced???

3.4.3.1 Extension to Higher Degrees of Freedom

Here we show that standard Jacobian Inverse manipulator control reduces to the controller described above.

In Jacobian Inverse control for a single manipulator, we calculate a desired velocity $\dot{\mathbf{x}}_d$ and a desired incremental tip motion $\tilde{\mathbf{x}}$ which will maintain our desired manipulator trajectory. We can combine these into a reference velocity $\dot{\mathbf{x}}_r$ using a factor of λ which represents the bandwidth of the trajectory command and should be designed to be within our positioning servo bandwidth:

$$\dot{\mathbf{x}}_r = \dot{\mathbf{x}}_d - \lambda\tilde{\mathbf{x}} \tag{3.13}$$

where

$$\tilde{\mathbf{x}} = \mathbf{x} - \mathbf{x}_d \tag{3.14}$$

Note that if the cartesian position is lagging the desired cartesian position, $\dot{\mathbf{x}}_r$ increases and if the cartesian position is leading the desired cartesian position, $\dot{\mathbf{x}}_r$ decreases. Thus position feedback is implicitly included in $\dot{\mathbf{x}}_r$. Then we convert our cartesian reference velocity into a desired joint velocity:

$$\dot{\mathbf{q}}_r = J^{-1}\dot{\mathbf{x}}_r = J^{-1}(\dot{\mathbf{x}}_d - \lambda\tilde{\mathbf{x}}) \tag{3.15}$$

Then we apply the following controller:

$$\boldsymbol{\tau} = -B(\dot{\mathbf{q}} - \dot{\mathbf{q}}_r) \tag{3.16}$$

which is effectively a joint space P.D. controller with velocity gain B and position gain λB.

For our two degree of freedom macro-micro slave manipulator, let $\mathbf{x}$ represent the cartesian output vector, let x_s represent the output cartesian position and let θ represent the orientation of the output link. Then $\mathbf{x} = [x_s \ \theta]^T$. Let $\mathbf{q} = [q_1 \ q_2]^T$ represent a vector of joint positions, then:

$$\dot{\mathbf{x}} = J\dot{\mathbf{q}} = \begin{pmatrix} \dot{x}_s \\ \dot{\theta} \end{pmatrix} = \begin{pmatrix} 1 & 1 \\ 0 & 1/l_2 \end{pmatrix} \begin{pmatrix} \dot{q}_1 \\ \dot{q}_2 \end{pmatrix} \tag{3.17}$$

where J is the manipulator Jacobian. Converting our cartesian reference velocity into a joint reference velocity we have:

$$\dot{\mathbf{q}}_r = J^{-1}\dot{\mathbf{x}}_r = J^{-1}(\dot{\mathbf{x}}_d - \lambda\tilde{\mathbf{x}}) = \begin{pmatrix} 1 & -l_2 \\ 0 & l_2 \end{pmatrix} \begin{pmatrix} \dot{x}_{sd} - \lambda\tilde{x}_s \\ \dot{\theta} - \lambda\tilde{\theta} \end{pmatrix} \tag{3.18}$$

We may substitute:

$$x_{sd} = q_3 \tag{3.19}$$
$$\tilde{x}_d = q_1 + q_2 - q_3 \tag{3.20}$$

and note that $\theta l_2 = q_2$ to get:

$$\mathbf{q}_r = \begin{pmatrix} q_3 - \lambda q_1 + \lambda q_3 \\ -\lambda q_2 \end{pmatrix} \tag{3.21}$$

Our slave controller is given by:

$$\begin{aligned} \boldsymbol{\tau} &= B(\dot{\mathbf{q}} - \dot{\mathbf{q}}_r) && (3.22) \\ \tau_1 &= -B(\dot{q}_1 - \dot{q}_3) - B\lambda(q_1 - q_3) && (3.23) \\ \tau_2 &= -B\dot{q}_2 - \lambda B q_2 && (3.24) \end{aligned}$$

The master is only one degree of freedom, so its controller is straightforward. Its desired position is simply the slave tip position so that its controller is given by:

$$\tau_3 = -K_3(q_3 - q_1 - q_2) - B_3(\dot{q}_3 - \dot{q}_1 - \dot{q}_2) \tag{3.25}$$

If we compare these equations to Equations 3.9, 3.11, and 3.12, we see that they are identical if we substitute $K_1 = \lambda B, K_2 = \lambda B, B_1 = B$, and $B_2 = B$. That is, we would prefer to tune the individual gains seperately in order to tailor them to our hardware. In reality the λ and gains required for each axis will be different due to differences in inertia, encoder resolution and friction. Low inertia axes naturally require lower gains than high inertia axes which can be taken advantage of to achieve force scaling. Force scaling is implemented by:

1. Designing the master and micro inertias in a ratio similar to the desired force scaling gains.
2. Tuning the gains for good position response.
3. Retuning the gains to achieve our desired force scale factor. If bandwidth limitations were uniform across all axes, then inertia would be the only factor affecting stiffness gains, and our gains would be in the ratio of our force scale factor. However in the presence of other factors such as encoder resolution, we must retune.

3.4.4 Modified Jacobian Inverse Controller

This method is what might be thought of as "traditional macro-micro control" because this approach was developed originally to increase response times of realtively slow and/or flexible industrial manipulators by adding a small, high bandwidth micro

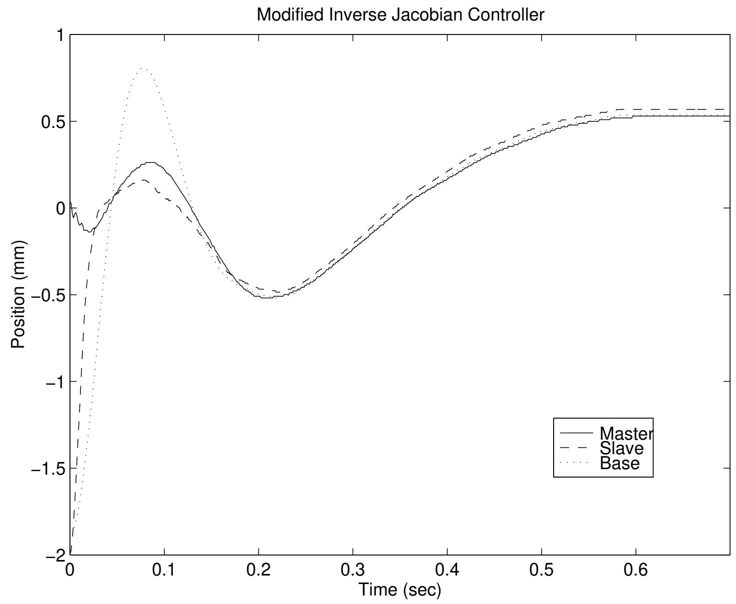

Figure 3-12: Step response for the master and slave using the Modified Jacobian Inverse control.

manipulator to the end. The idea, which has been used by (Sharon et al., 1993), is to command the micro actuator to null error between the master position and macro position. If the micro actuator has a faster servo bandwidth than the macro actuator, then it will tend to "jump out ahead" of the macro actuator and consequently decrease position response times. Its effect on a teleoperator system is discussed below.

The controller is given as follows. As before, the master desired position is that of the slave tip:

$$\tau_3 = -K_3(q_3 - q_1 - q_2) - B_3(\dot{q}_3 - \dot{q}_1 - \dot{q}_2) \tag{3.26}$$

The macro desired position is equal to that of the master so that:

$$\tau_1 = -K_1(q_1 - q_3) - B_1(\dot{q}_1 - \dot{q}_3) \tag{3.27}$$

Now the micro position is not servoed to zero, but rather directly to the master position:

$$\tau_2 = -K_2(q_2 - q_3 + q_1) - B_2(\dot{q}_2 - \dot{q}_3 + \dot{q}_1) \tag{3.28}$$

This is what gives the "jump out ahead" behavior to the micro axis.

Figure 3-12 shows the 2 mm step response for this controller. The gains used were:

$$\begin{array}{ll} K_1 = 7000 \text{ N/m} & B_1 = 55 \text{ Ns/m} \\ K_2 = 160 \text{ N/m} & B_2 = 1.3 \text{ Ns/m} \\ K_3 = 8000 \text{ N/m} & B_3 = 65 \text{ Ns/m} \end{array}$$

The position of the micro is the difference between the curves labelled Slave and Base. The micro initially jumps out ahead of the base (macro) axis. The master does not move a great deal because while the position of the slave tip is negative, its velocity is large and positive. The effects cancel in the master P.D. controller, and as a result, most of the relative motion between the master and slave is caused by the slave which generates substantial momentum. The base overshoots the position of the master while the micro compensates by reversing its direction and tracking the master. The micro effectively locks on to the master position.

However the master is not a fixed target. In fact, it tracks the slave and begins to oscillate with it as they both settle. The result is the overall amount of oscillation is greater due to the added control input caused by the micro actuator. The overall speed of response is roughly 10 times slower than in the previous Jacobian Inverse control case.

The additional oscillation present in the response is more striking in Figure 3-13, the Modified Inverse Jacobian contact response plot. The contact in this case is barely stable. The slave tends to bounce on the surface of the aluminum block. This is because the master, which is tracking the slave, tends to overshoot slightly and the micro actuator now wants to track these oscillations. Of course the master tries to track the master oscillations, and the macro tracks the master. Considerable energy is added to the system at this point because the master and macro use much higher gains, hence much larger torques are applied. The fact that the micro axis is directly coupled to the master and macro and reacts to them is critical and causes this behavior. In the previous Jacobian Inverse control, the master and macro track the micro, but the micro does not track them; it simply tries to settle to zero so that a loop does not form in which energy can increase.

We can decrease the overall stiffness gains in order create overdamped responses in order to stabilize the system, but this in turn reduces the overall stiffness of the master-slave connection. The increase in the level of oscillation in the system and the poor contact response make this method of control far less desirable than the previous Inverse Jacobian control.

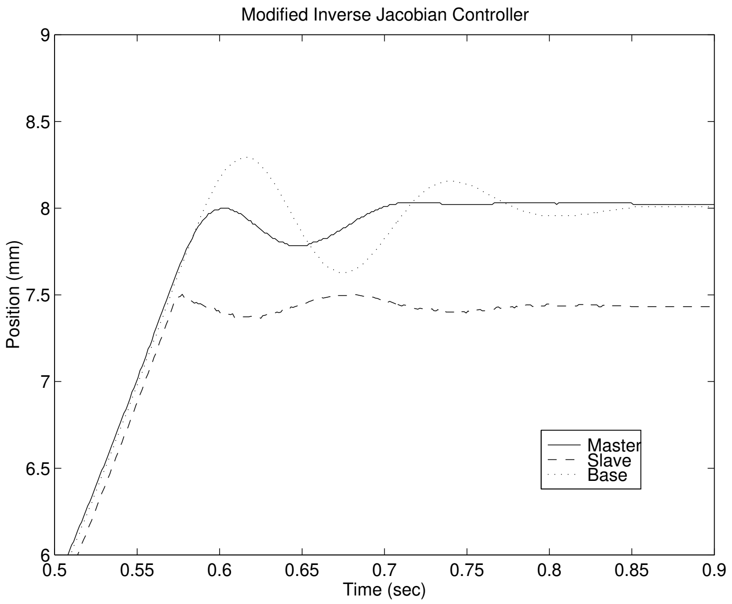

Figure 3-13: Contact response for the master and slave using the Modified Jacobian Inverse control.

3.4.5 Simulated Force Sensor Controller

A popular method to implement teleoperator force reflection is to use a distal force sensor on the end of the slave manipulator and to feed these forces directly back to the master. The master then tracks the endpoint position of the slave. So it is natural to ask how our system would perform if we were to use the micro actuator simply as a force sensor. In this case, we command the micro actuator to remain at zero:

$$\tau_2 = -K_2 q_2 \tag{3.29}$$

We feed this force back to the master:

$$\tau_3 = -\tau_2 \tag{3.30}$$

And we command the macro to track the master:

$$\tau_1 = -K_1(q_1 - q_3) - B_1(\dot{q}_1 - \dot{q}_3) \tag{3.31}$$

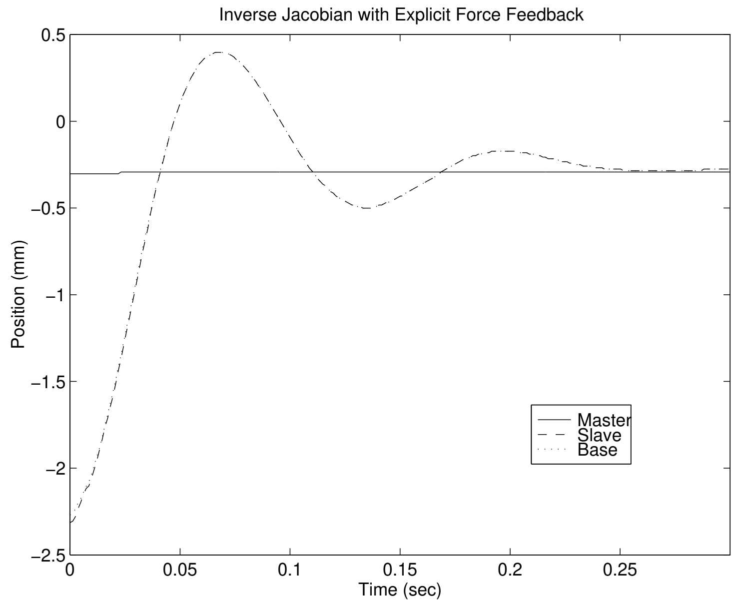

Figure 3-14: Step response for the master and slave using a simulated force sensor controller.

The gains were chosen as before to give 50:1 force scaling.

$$\begin{array}{ll} K_1 = 7000 \text{ N/m} & B_1 = 55 \text{ Ns/m} \\ K_2 = 163.74 \text{ N/m} & B_2 = 1.331 \text{ Ns/m} \\ K_3 = 8000 \text{ N/m} & B_3 = 65 \text{ Ns/m} \end{array}$$

The 2 mm step response for this system is shown in Figure 3-14. Because there is no contact being made with the micro actuator in this freespace motion, no forces are commanded to the master. The micro also does not move relative to the macro. The base (macro) compensates entirely on its own and eventually reaches the master position in a classic second order response. When contacting a rigid surface, the slave displays classic contact instability as shown in Figure 3-15. Because the contact force is fed directly back to the master, the master is forced backwards away from the block. The macro axis tracks this motion and pulls the entire slave away from the aluminum block. But the user is still pushing the master towards the block, so it reinitiates contact. A violent increase in the amplitude of the oscillations occurs.

This behavior can of course be avoided by reducing gains. But then the same level of force reflection cannot be achieved as with other methods, in particular the Jacobian Inverse method. Another way of looking at this problem is that while the slave is in contact with the aluminum block, a very high position gain exists between

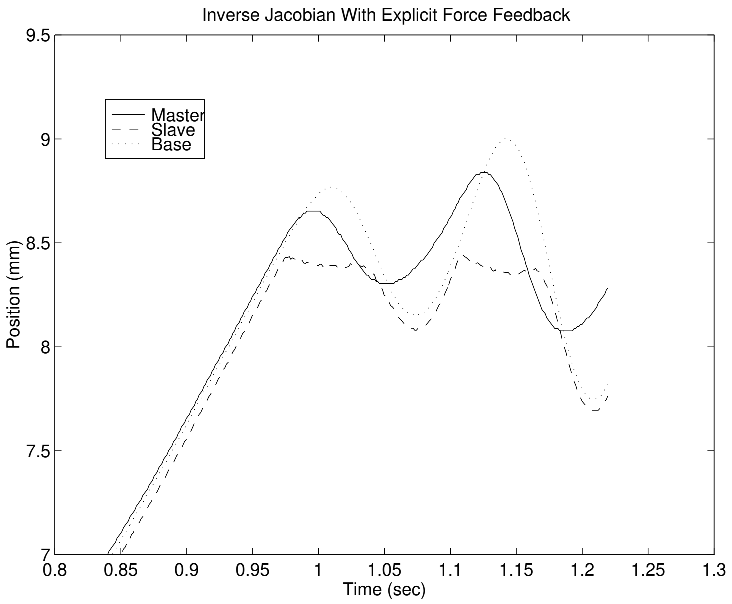

Figure 3-15: Contact response for the master and slave using a simulated force sensor controller. Note the classic contact instability.

the micro position and torques applied to the master. Very small position changes in the micro actuator creates forces which are amplified by the 50:1 force scaling and sent back to the master. This in turns causes rapid movement of the master which the slave is then forced to track. The result is clearly undesirable.

3.4.6 Friction Instability

There is one other phenomenon which I would like to point out that is common to several of the controllers presented, though in varying degrees. First note that the Inverse Jacobian, Modified Inverse Jacobian and Simulated Force Sensor controllers all use deflections in the micro position to generate force commands to the master axis. Any static friction in the micro actuator will cause a fixed non-zero deflection which is indistinguishable from an actual force. Any of the above controllers will react by commanding torques to the master and macro axes. If these torques overcome the static friction in these axes, the master and macro axes will move, and the system will slowly "walk" until it contacts something and stops. The higher the force scale factor, the more likely that a fixed micro deflection will result in torques which will move the master and macro axes.

Now if the slave tip is placed between two rigid surfaces, an oscillation can develop.

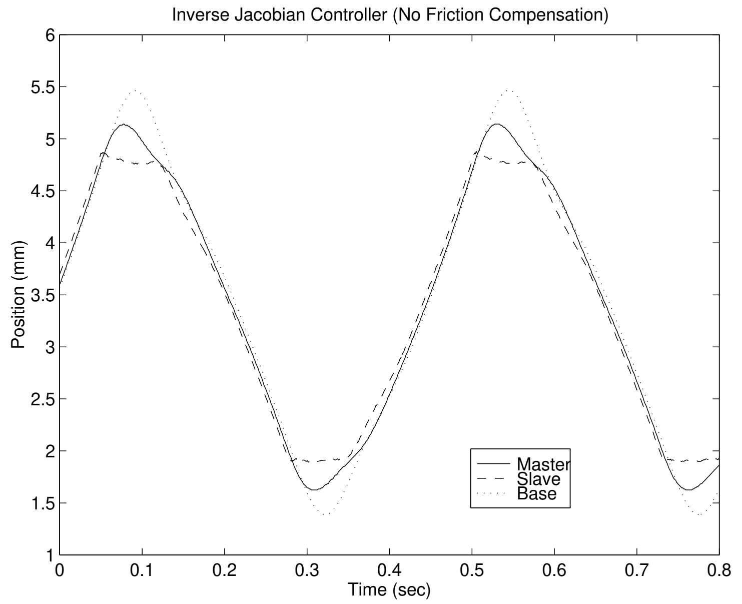

Figure 3-16: A friction induced osciallation using Jacobian Inverse control with friction compensation turned off. The slave oscillates by slowly bouncing between two aluminum blocks.

If the slave bumps one surface, the micro axis will “flip” through its zero point and get stuck in its friction in the opposite direction. As a result it will move towards the second rigid surface, bump into it, flip back through its zero position, and move towards the first surface. The result is an oscillation which sounds like a clock ticking.

Recall that a joint level friction compensation algorithm was running on all axes during all of the above tests. This effectively lowers the size of the fixed micro deflection. In the case of the Jacobian Inverse controller, this behavior did not develop in our tests with the friction compensation running. However with it off, we could create oscillations between two rigid surfaces like that shown in Figure 3-16. The Modified Inverse Jacobian control would exhibit similar behavior when friction compensation was turned off, Figure 3-17. The Simulated Force Sensor control exhibited this behavior even with friction compensation turned on, as shown in Figure 3-18, and became unstable if friction compensation was turned off, Figure 3-19.

3.4.7 Summary

The idea of using a slave manipulator with macro and micro degrees of freedom which can be used in conjunction to reduce endpoint inertia and improve force reflection is

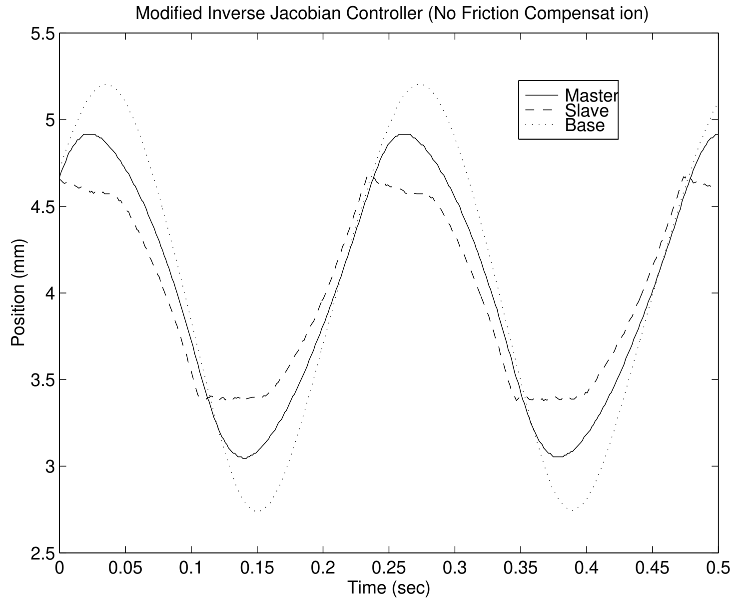

Figure 3-17: A friction induced osciallation using Modified Jacobian Inverse control with friction compensation turned off. The slave oscillates by slowly bouncing between two aluminum blocks.

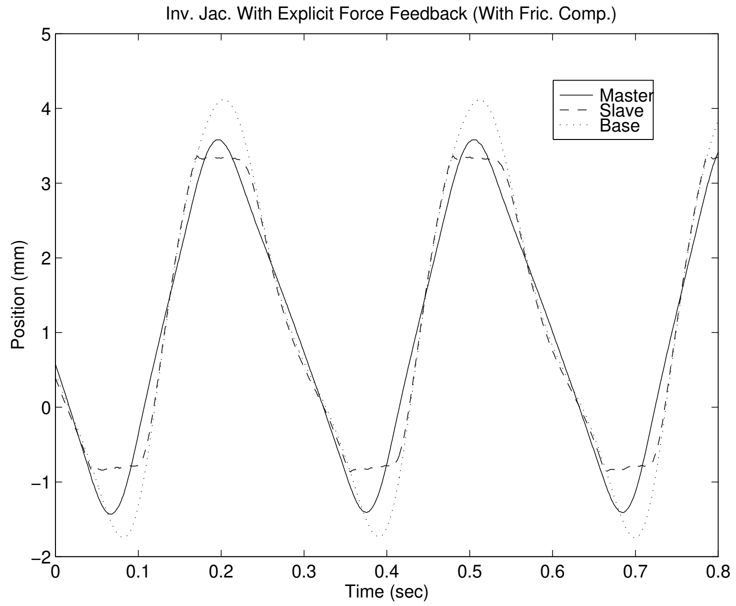

Figure 3-18: A friction induced osciallation using Simulated Force Sensor control with friction compensation turned on. The slave oscillates by slowly bouncing between two aluminum blocks.

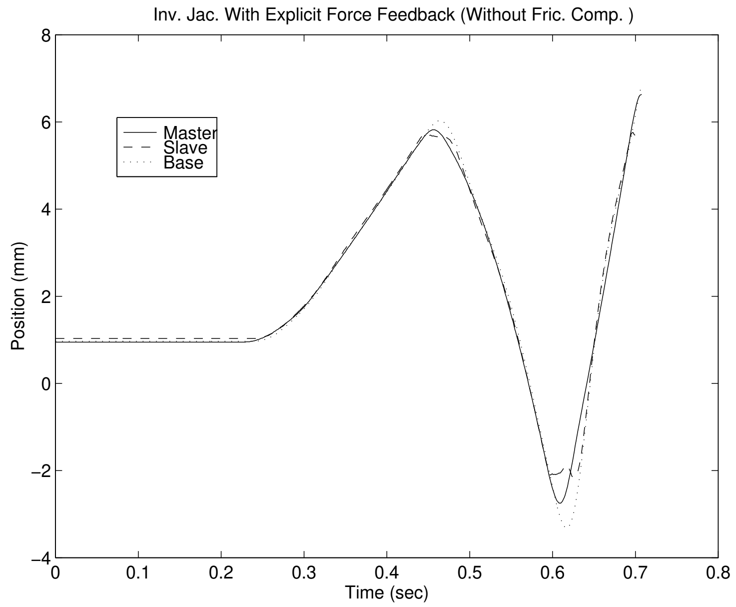

Figure 3-19: A friction induced osciallation using Simulated Force Sensor control with friction compensation turned off. The slave oscillations increase catastrophically.

good, but nontrivial to implement. Of the methods that we tried, we found that an Inverse Jacobian type approach yielded the best results. Motions in freespace in fact felt free. The user could feel the inertia of the master, and an inertia due to movement of the micro axis, but the inertia of the macro axis was essentially hidden. Contacts felt crisp, and remarkably small and soft objects such as erasers and tissue paper could be made to feel heavy and rigid using a force scaling of 50:1. Such behavior existed over the larger workspace of the macro axis.

However friction and inertia in the micro axis were also scaled by a factor of 50. The inertia and friction were not very noticable using our system, but the absolute values in our system were miniscule by most robot standards. Our friction was dominated by brush friction and was only 0.02 N at the tip of the micro axis. This kind of low friction is not to be expected in a larger manipulator. The level of force reflection and force scaling will be directly limited by the end effector friction levels which we can achieve when using this approach.

3.5 Implications for Teleoperator Design

Prior to this investigation, I had believed that the limitations imposed by our use of the basic force reflecting teleoperator, described in Chapter 2 and earlier in this chapter in Section 3.4.1, would prevent us from achieving force reflection without a force sensor. If we were to use only the basic force reflecting teleoperator control, we would conclude that:

- The slave must be very light in order to allow force reflection. Too much inertia will simply overly attenuate force information being conveyed to the user.
- Force scaling where forces are increased to the user would make things even worse. If the slave has a large inertia, such scaling will make it feel even heavier, as we saw in this chapter using the Jacobian Transpose controller.
- Disturbances caused by tissue forces at the incision point disturbances would be felt directly by the user.
- The only real option to make the slave feel lighter is to use a force sensor between the slave and the environment. This has its own set of problems as discussed in Chapter 2 and in this chapter in Section 3.4.5, and furthermore inertia reduction would be limited to low bandwidths.

However, in our simple macro-micro testbed, we find that:

- The slave can have a heavy base corresponding to the macro actuator (which will ideally carry all the heavy components like motors) and still achieve good force reflection. The base can have friction and other disturbances which the user will feel very little of.
- The user will feel only the intertia of the end effector, corresponding to the micro actuator, but this is very low. If forces are scaled up, the effect of this inertia will be correspondingly greater, but if the end effector can be made sufficiently light, this would not be an issue. In this testbed, the end effector inertia is very small, that of a small aluminum "T" and the motor rotor inertia.
- Probably the most severe constraint is caused by the fact that the user will feel friction in the end effector. We will find this constraint severe because due to our desire to miniaturize, this is precisely where friction is difficult to eliminate. In our testbed, the only friction was due to motor brushes and was very small. However, we will find that in the design of a 3 or 4 degree of freedom end effector, minimizing friction becomes a considerable challange.

- We note that the "right" scaling to have depends on the relative inertias of different components of the system. Since gains can be made higher on higher inertia degrees of freedom, the inertias to some extent dictate the type of scaling possible. Conversely, if we desire a certain type of scaling, the inertias should be designed correspondingly. In the case of the testbed, the master inertia was 200 times larger than that of the micro actuator. The result was that a 50:1 force scaling was achievable and felt quite good.[2]

We will see that the hard part of the design is the incorporation of a wrist whose primary purpose is to give the added dexterity that we want to allow tasks like suturing, *and* which satisfies the properties of our testbed's one DOF end effector. If it does however, we should be able to achieve force reflection in a system several orders of magnitude heavier than we previously thought possible. The design of the wrist now becomes doubly important since we give it the responsibility of enabling force reflection.

Up to this point, we have focussed entirely on forces, and not on torques, applied to the end effector. We are going to continue in this way though this is not a limitition in this approach. The reason is that our master, the Phantom, only allows us to feel forces. This is not necessarily a bad thing. We have found that in virtual environments, forces alone can create compelling illusions that the user is touching virtual objects and surfaces, both rigid and deformable. One of the things we will learn is that torque information can be useful for some tasks, but for a first system, this is not at all necessary, even for a surgical teleoperator master.

We conclude this chapter by proposing the following hypothesis, which we will explore as we design and test the two systems described herein, the Silver Falcon and the Black Falcon: We propose that we can use a wrist to achieve orientation degrees of freedom for the system and at the same time allow redundant positional degrees of freedom to enable macro micro force control of a point at the tip of the end effector. We will pursue this idea further in the next chapter.

[2]We could program a higher force scale factor but the resulting slave stiffness would be unacceptably low. In principle, we could also increase the master stiffness, but limitations in master encoder resolution prevent this.

Chapter 4

Design Goals and Constraints

In this chapter, we discuss specific goals and constraints which affect the slave manipulator designs presented in Chapters 5 and 6. We ask:

- What type of kinematics, how many degrees of freedom, and what range of motion do we need in order to provide dexterity for surgery?
- How must the kinematics of the slave manipulator be constrained in order to perform minimally invasive surgery?
- How does our undertanding of teleoperator control developed in the previous chapters affect the desired kinematics and dynamics of our design?
- How will practical issues regarding use in the operating room affect the overall structure of the design?

In this chapter, we focus on the slave manipulator, however the design of the teleoperator *master* is obviously an important aspect of the overall system design. In our work, we will use a modified Phantom™ haptic interface (Massie and Salisbury, 1994) to control both slave manipulators which we present. Though we do not present a new master design in this thesis, we will discuss desirable attributes for a master to possess in Chapter 7.

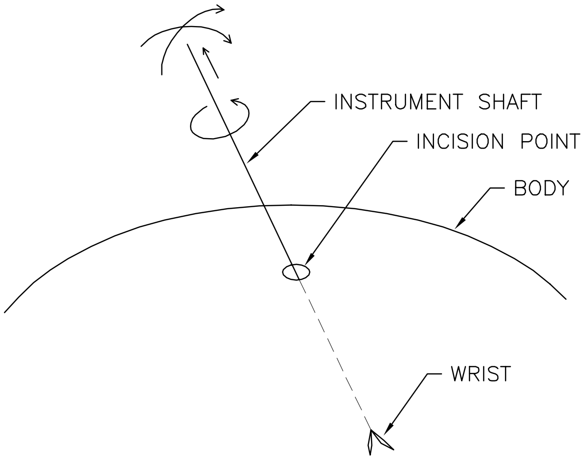

Figure 4-1: The incision point constrains the motions of one link of the slave manipulator to four degrees of freedom.

4.1 Kinematics Requirements

4.1.1 The Incision Point Constraint

A fundamental requirement of MIS is that the instrument must pass through a small incision when entering the body, as shown in Figure 4-1.

If we imagine that some portion of the slave consists of a shaft which passes through the incision point, this shaft will be constrained to have a maximum of four DOF. Considering that we wish the surgeon to perform as though they were performing open surgery, the tip of the slave manipulator we design should have at least six DOF plus one gripping freedom, or seven total. In order to achieve seven total DOF, an additional three DOF mechanism must be placed distally to the incision site (inside the patient). We feel this is best done using a compact wrist mechanism that will not get in the way of other instruments or tissue structures at the operating site. Such a wrist has a number of fairly severe requirements:

- The wrist must have sufficient and appropriate degrees of freedom to allow specific surgical tasks such a suturing.
- The wrist must support substantial loads in order to grip needles and to manipulate tissue.
- When used in conjunction with the control methods discussed in Chapter 3, such a wrist should also help us achieve force reflection by acting as a micro

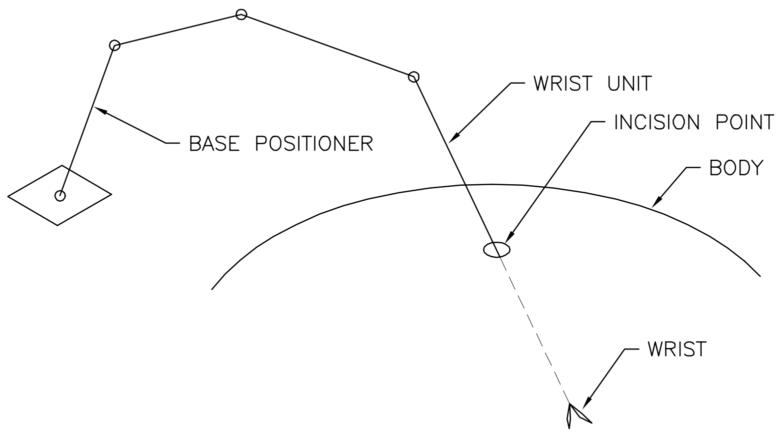

Figure 4-2: The kinematic constraints on the slave manipulator defines its overall structure. While many other general concepts could be formulated (snake robots, robots which assemble through multiple ports), a slave manipulator which consists of a wrist unit coupled to a base positioner is straightforward and will prove effective.

actuator, and must have the appropriate dynamics to do so.

The wrist and accompanying mechanism will be referred to as the wrist unit. The wrist unit must naturally be carried by the remainder of the slave manipulator and postioned relative to the surgical site. The overall structure for the slave manipulator is shown in Figure 4-2. We will refer to the portion of the slave manipulator which carries the wrist unit as the base positioner.

4.1.2 Suturing Motions

Consider the task of suturing, Figure 4-3. (Hunter and Sackier, 1993) suggest the proper positioning of an MIS needle driver with respect to the tissue which must be approximated (sutured). The needle driver should be in a plane vertically above the suture line, and nearly parallel (within 20 degrees) to the tissue. The motion required to suture is largely a rotation about the instrument shaft, combined with a push to drive the needle through the tissue. The tissue may be held with another instrument.

In the absence of a wrist, the orientation of the instrument with respect to the suture line defines the point of entry into the body of the tool. The tissue may be moved to orient the suture line with respect to the tool, but this is not always possible. If the suture line is rotated by 45 degrees with respect to the orientation shown in the figure, then it will be difficult to maintain proper needle orientation. However, a wrist which could reorient by 45 degrees could maintain the correct needle orientation

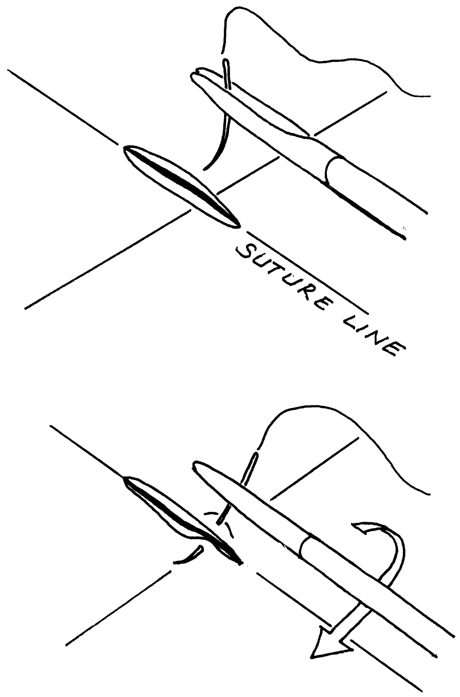

Figure 4-3: The proper positioning of a needle driver with respect to tissue is critical during suturing. Suturing is primarily a rolling motion combined with a push in the direction the needle is driven. Adapted from (Hunter and Sackier, 1993).

during the suturing motion.

Maintaining such an angle would realistically require more range of motion than ±45 degrees. An educated estimate is that the advantages of having a wrist will probably not be worth the substantial design effort involved unless ±90 degree movements are possible. On the other hand, bending at much more than 90 degrees will likely not be useful given that the wrist would then begin to interfere with the instrument shaft on which it is mounted.

4.2 Wrist Kinematics

Wrist design is a subject unto itself as demonstrated by the many robotic wrists which have been designed. By way of example, we discuss just a few wrist kinematics options below in order to give an idea of the relevant issues involved.

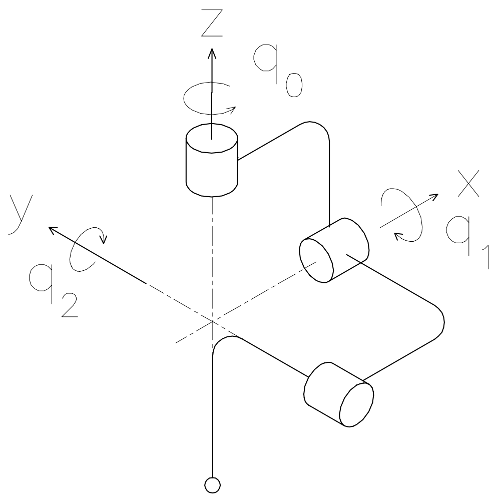

Figure 4-4: Kinematics for a roll-pitch-yaw wrist. The small circle at the lower tip of the structure represents a point where objects might be held by a gripper mounted distally on the wrist.

Note that there are many more issues involved with actually implementing any of these kinematic types concerning structure, actuation, transmisions, sensing and so forth. These types of issues are addressed only within the context of the designs we present in Chapters 5 and 6.

4.2.1 Roll-Pitch-Yaw

The shape of an instrument which must pass through an incision might naturally include a long slender shaft. If so, it is natural for the first axis of the wrist to be a rotation about this instrument shaft. If we use the motions for suturing as a guide, a rolling motion seems to be required at the output where the needle is held. One way to do this is through a universal (cardan) joint as used in automotive drive shafts. In this case two intersecting, perpendicular axis are located near the end of the instrument shaft to give the pitch and yaw axes.

This results in a roll-pitch-yaw wrist are shown in Figure 4-4. Roll-pitch-yaw refers to the orientation of revolute joints from the base of the wrist moving outwards towards the tip.

4.2.1.1 Angular Velocity Singularities

Singular configurations are a common problem in wrist design. The traditional differential kinematics mapping between a manipulator joint velocities $\dot{\mathbf{q}}$ and the angular and/or linear velocity of a point on the manipulator $\dot{\mathbf{x}}$ (typically of the end-effector) is:

$$\dot{\mathbf{x}} = J\dot{\mathbf{q}} \tag{4.1}$$

where J is the manipulator Jacobian matrix whose elements are a function of its configuration $\mathbf{q}$. The manipulator is said to be *singular* in configurations where J loses rank. In this case, a manipulator consisting of serially connected links will require infinite joint velocites to produce certain output velocities which are hence impossible. If:

$$\omega = \begin{pmatrix} \omega_x \\ \omega_y \\ \omega_z \end{pmatrix}, \ \dot{\mathbf{q}} = \begin{pmatrix} \dot{q}_0 \\ \dot{q}_1 \\ \dot{q}_2 \end{pmatrix} \tag{4.2}$$

are vectors of angular velocities about the coordinate frame axis, shown in Figure 4-4 and joint velocities respectively, then:

$$\omega = J\dot{\mathbf{q}} = \begin{pmatrix} 0 & c_0 & -s_0c_1 \\ 0 & s_0 & c_1c_0 \\ 1 & 0 & s_1 \end{pmatrix} \dot{\mathbf{q}} = \begin{pmatrix} \hat{\mathbf{q}}_0 & \hat{\mathbf{q}}_1 & \hat{\mathbf{q}}_2 \end{pmatrix} \dot{\mathbf{q}} \tag{4.3}$$

where $\hat{\mathbf{q}}_i$ is a unit vector along the ith joint axis. If q_1 is rotated by $\pm\pi/2$

$$J = \begin{pmatrix} 0 & c_0 & 0 \\ 0 & s_0 & 0 \\ 1 & 0 & \pm 1 \end{pmatrix} \tag{4.4}$$

Since $\hat{\mathbf{q}}_0$ and $\hat{\mathbf{q}}_2$ are parallel, rank$(J) = 2$, and we lose the ability to roll the output of the wrist.

Consider suturing as described above. The primary motion is a rolling motion. As a result, we expect that suturing will become essentially impossible for a roll-pitch-yaw wrist near its singular configurations.

If the range of motion of joints 1 and 2 are $\pm\pi/2$, then the workspace of the wrist is a hemisphere and the two singular points at $q_1 = \pm\pi/2$ are at the edges of the wrist workspace. If singularities do exist, having them at the edges of the workspace is beneficial.

4.2.1.2 Linear Velocity Singularities

We may also consider the mapping between joint velocities and linear velocities of a point on the last link of the wrist such as the small circle shown in Figure 4-4. Let $\mathbf{x}$ be a vector along the last link from the intersection of the three joint axes to this point. Then:

$$\dot{\mathbf{x}} = \begin{pmatrix} \mathbf{x} \times \hat{\mathbf{q}}_0 & \mathbf{x} \times \hat{\mathbf{q}}_1 & \mathbf{x} \times \hat{\mathbf{q}}_2 \end{pmatrix} \dot{\mathbf{q}} \tag{4.5}$$

In this case, $\mathrm{Rank}(J) = 2$ for all values of q_0, q_1 and q_2 because all the columns are orthogonal to $\mathbf{x}$. It is impossible to produce a velocity $\dot{\mathbf{x}}$ in a direction along the last link, that is along a vector $\mathbf{x}$.

If the wrist is mounted on a larger arm, this lack of mobility is traditionally not a problem. However recall that the macro-micro control described in Chapter 3 requires there be redundant degrees of freedom in the directions which we would like force reflection. Since this wrist is always singular with respect to positions in one direction, macro-micro control would only provide force feedback in two of three directions when used with a roll-pitch-yaw wrist.

4.2.2 Roll-Pitch-Roll

Another common set of wrist kinematics is roll-pitch-roll, shown in Figure 4-5. This wrist is similar to a roll-pitch-yaw wrist with the final link rotated by $\pi/2$.

4.2.2.1 Angular Velocity Singularities

Just as in the roll-pitch-yaw wrist, there are two singularities when q_1 is rotated by $\pm\pi/2$ from the orientation shown in the figure.

Again, when singular, angular velocities can only be produced in the plane formed by the axes of joints 0 and 1. The wrist is farthest from its singularities when q_1 is in the orientation shown in the figure, so the wrist therefore operates optimally at a right angle.

The advantage of this wrist is that the output roll which is so critical for suturing is always available. The instrument shaft would ideally be inserted into the body perpendicular to the tissue being sutured instead of parallel to it as in the case of no wrist or the roll-pitch-yaw wrist.

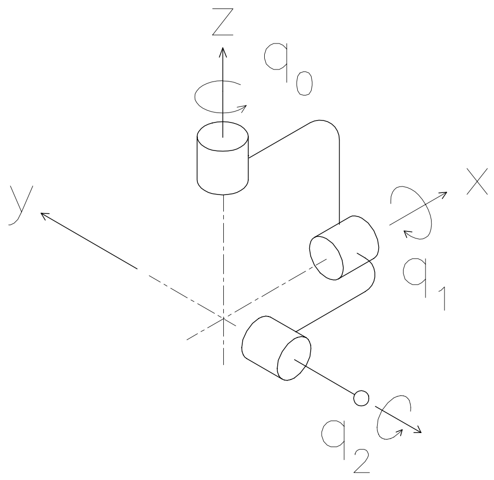

Figure 4-5: Kinematics for a roll-pitch-roll wrist. The small circle at the lower tip of the structure represents a point where objects might be held by a gripper mounted distally on the wrist.

4.2.2.2 Linear Velocity Singularities

The roll-pitch-roll wrist is also singular with respect to linear velocities for all q_0, q_1, and q_2 just as is the roll-pitch-yaw wrist. That is, linear velocities are impossible in a direction along the last link, again making macro-micro control impossible in this direction. However, when q_1 is rotated by $\pm\pi/2$, linear velocities also become impossible along $\hat{\mathbf{q}}_1$. So always having output roll available does come at a cost.

4.2.3 Roll-Pitch-Yaw-Roll

In an effort to avoid singularities, more joints can be added. Consider the roll-pitch-yaw-roll wrist shown in Figure 4-6. This wrist avoids angular velocity singularities (losing output roll) by adding an extra roll degree of freedom on the distal link. This can be effective, but we should note that singularities can still be found. A singular configuration for this wrist is shown in Figure 4-7

The interesting point is that by reorienting q_1 by $\pi/2$, this singular configuration can be avoided while maintaining the same output link orientation. In fact, we can always (ignoring joint range of motion limits) use the redundant degree of freedom to avoid angular velocity singularities. One must be careful when resolving this type of redundancy in a 4R wrist (a wrist with four interecting revolute joints) because the wrist configuration will be dependent on the path by which the output link reaches its orientation. This is discussed in (Long et al., 1989)

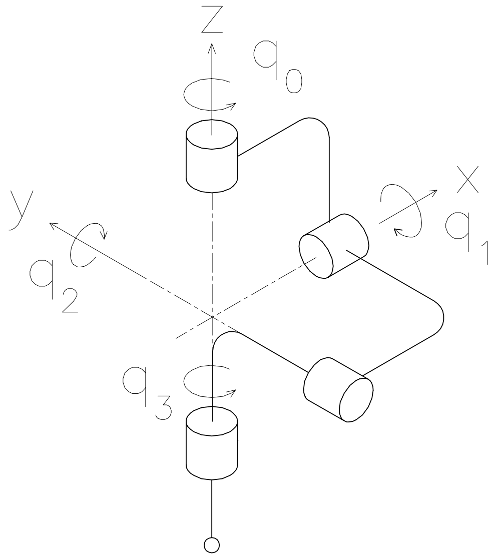

Figure 4-6: Kinematics for a roll-pitch-yaw-roll wrist. The small circle at the lower tip of the structure represents a point where objects might be held by a gripper mounted distally on the wrist.

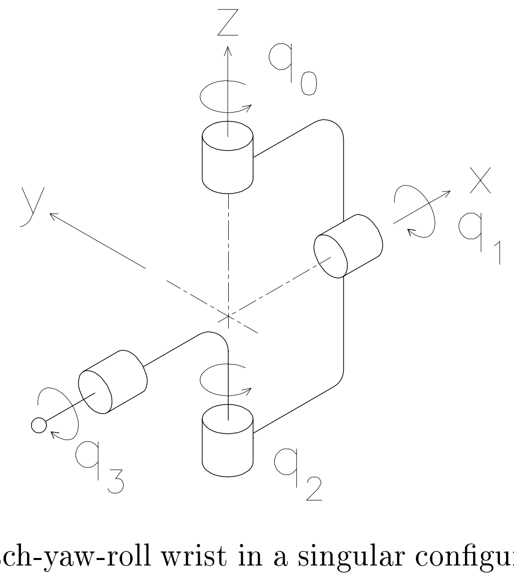

Figure 4-7: The roll-pitch-yaw-roll wrist in a singular configuration. All joint axes lie in a plane. Angular velocities out of the plane are impossible.

A redundant wrist of course has the disadvantage of adding an actuator which we might not otherwise need, and further increasing design complexity.

4.2.3.1 Rosheim

Deserving an "interesting mention" is a variation of the roll-pitch-yaw wrist known as the omni-wrist, which has no angular velocity singularities, (Rosheim, 1989) This wrist is difficult to describe but consists essentially of a pair of cardan joints linked in series. The redundant two degrees of freedom are resolved internally to the wrist using a fairly complicated set of gears and rollers so that each bends half of the total reorientation of the wrist. At a wrist limit of 90 degrees, each cardan joint reorients by than 45 degrees so they remain non-singular. Output roll is fed through the wrist using a smaller double cardan driveshaft. While such a complex wrist is difficult to miniaturize, (Schenker and Charles, 1995) describes a Rossheim variant designed at the Jet Propulsion Lab which has an approximately 2.5 cm outside diameter.

4.3 Base Kinematics

The slave manipulator must be designed so that one link always passes through a constrained point, the incision point. The three most logical ways for this to be done are to use 1) controlled redundant kinematics, 2) passive redundant kinematics, and the option which we choose, 3) remote center kinematics.

4.3.1 Controlled Redundant Kinematics

Consider an six DOF robot whose last link is a rigid shaft. If the manipulator is not in a singular configuration, the shaft will have six DOF. Singular configurations of a manipulator (singularities) are configurations where the Jacobian matrix relating endpoint velocities to joint velocities becomes singular, or loses rank. If we wish to constrain a point on the shaft such that it does not translate, then we write the transformation between $n > 6$ joint velocities, $\dot{\mathbf{q}}$ and three linear and three rotational velocities of the point in consideration on the shaft $\dot{\mathbf{x}}$ and $\dot{\theta}$ respectively:

$$\begin{pmatrix} \dot{\mathbf{x}} \\ \dot{\theta} \end{pmatrix} = J\dot{\mathbf{q}} \tag{4.6}$$

If we set:

$$\dot{\mathbf{x}} = \mathbf{v} \tag{4.7}$$

where **v** is a vector representing the desired velocity and points in a direction along the axis of the shaft, then the equations above represent a constraint on joint velocities which enforce the incision point constraint.

We therefore constrain the robot to act like a four DOF robot to satisfy the incision point constraint. If additional freedoms are incorporated so that the end-effector has six degrees of freedom plus a gripping freedom after the constraint is applied, then the robot will have a minimum of nine DOF.

There are two disadvantages to this approach:

- The addition of redundant actuators and degrees of freedom is costly and wasteful if unnecessary. It is our experience that the complexity of a design can increase sharply with increased DOF and should be avoided if possible.
- We are effectively creating a two degree of freedom gimbal in software using this approach. The structural rigidity of this gimbal is therefore limited by the servo gains we can generate. Servo controlled joints are typically less stiff than actual mechanical bearings, so it is likely that some flexibility will be introduced between the manipulator base and its tip resulting in innaccuracy of motion and placing a limit on the stiffness of the connection between the master and slave manipulators.

4.3.2 Passive Redundant Kinematics

We could alternatively design redundant DOF into the robot which are uncontrolled; they freely rotate/translate in bearings. Instead of resolving the redundancy actively, we would let the cannula and tissue at the incision point passively constrain these redundant freedoms. This alternative uses the body to constrain the motion of the robot. The approach has the advantage of appearing simple and requires only as many actuators as degrees of freedom being controlled. Again, however the approach has several disadvantages:

- The body is soft and movable, and any movement of the body will result in uncontrolled motions of the robot tip. Forces applied at the tip of the manipulator will react against the body wall causing deflections which may be unwanted.
- We may use sensors in the uncontrolled joints and use the manipulator forward kinematics to find the manipulator tip position. We may then control the remaining joints in order to maintain a desired endpoing position and orientation.

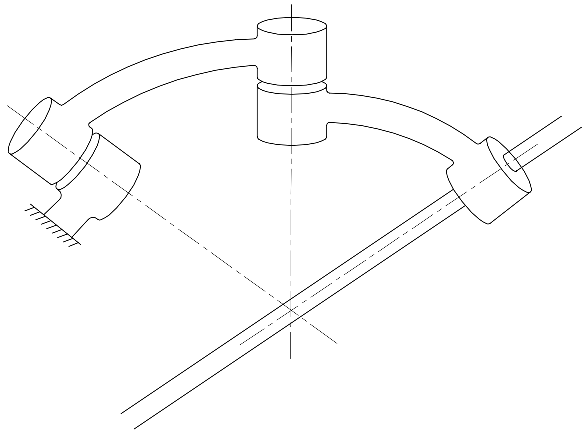

Figure 4-8: A serial linkage whose joint axis intersect at a single point will create spherical (remote center) motion.

> This is a case of non-colocated control where the actuators (the slave manipulator motors) and sensors (effectively the endpoint of the robot) are separated by flexibility introduced by the body wall (Sharon, 1988). It is well know that this is an inherantly unstable type of control with bandwidth being limited to well below the natural frequency of the "spring" introduced by the body wall.

4.3.3 Remote Center Kinematics

Our third option is to design a device with no redundant freedoms which, by its kinematic design, always places a part of the robot (the axis of a distal instrument shaft) through the incision point. Such devices exist and are called remote center devices, because they produce a remote center of rotation, unencumbered by mechanism, which can be placed at the incision point. This is the approach which we chose. We use the double parallelagram linkage described below, as further described in Chapter 5,

4.3.3.1 Spherical Linkages

One way of implementing a remote center is to use a spherical linkage such as that shown in Figure 4-8. If a serial linkage of revolute joints is designed such that its axes intersect at a single point, then the links rotate on a sphere about a remote center of rotation. If a shaft were to be placed in the second link as shown in the figure, it would be constrained to pass through the remote center.

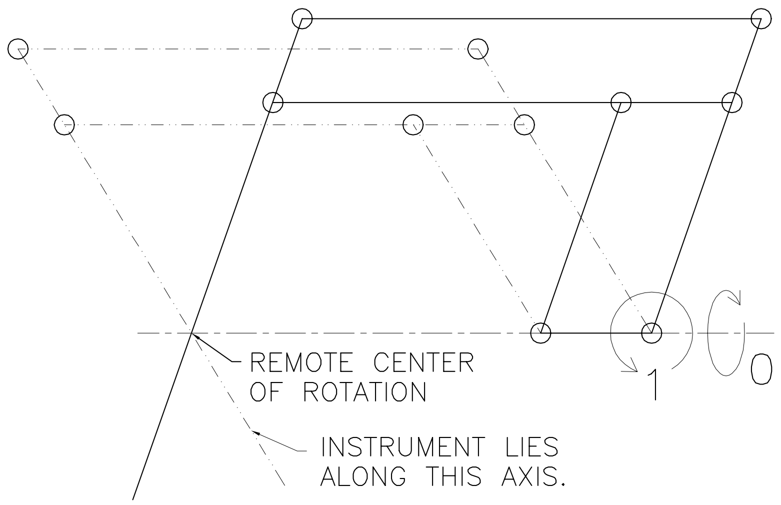

Figure 4-9: The double parallelagram remote center linkage. The circles represent revolute joints whose axes are perpendicular to the page. Axis 0 rotates the linkage out of the plane of the page.

We can imagine other combinations of linkages with the same property. Linear bearings might also be designed with curved bearings surfaces to follow the surface of a sphere again providing a remote center of rotation.

4.3.3.2 Double Parallelagram

Figure 4-9 shows the double parallelagram mechanism. A similar linkage is described separately in (Hamlin and Sanderson, 1994), (Taylor et al., 1995), and variations are commonly used in interior cabinet hinges. By combining two parallelagram linkages we can produces a remote center of rotation in a plane. By rotating the entire linkage out of the plane about the axis labelled 0, a spherical remote center is achieved.

This mechanism has several advantages as we will see in Chapters 5 and 6.

- Because the mechanism is essentially planar, mechanizing it is relatively straight forward.
- It is possible to run mechanical transmission cables along a planar linkage, making it possible to actuate the wrist unit using motors placed on a remote location of the linkage.
- The linkage may be gravitationally counterbalanced.
- The linkage has a natural way of extending over the patient.

4.4 Dynamics

At this point, we turn toward dynamic constraints on our system. Here we comment on the type of dynamics which we would like to see in the slave manipulator. These recommendations are a direct result of our experimentation with teloperator control, and macro-micro control in particular, as discussed in Chapter 3.

4.4.1 Wrist Dynamics

The wrist dynamics become important when we consider force reflection. If our goal was to only provide additional degrees of freedom to the surgeon, dynamic constraints would be far less important.

4.4.1.1 Wrist Inertia

Macro-micro control dictates that the inertia of the micro freedoms, in this case the wrist, be low. This is the portion of the robot that interacts with the environment and defines how the slave will appear, dynamically, to the user. Because of the small size of the wrist however, this is not a problem. In fact, the inertia of the motor rotors may be on the order of the wrist and gripper components.

We do however have a lower limit on the mass of the wrist components and their actuators which is dictated by the servo stiffness we wish to achieve. We may reduce the mass until achieving a desired servo stiffness becomes impossible given bandwidth limitations on our system, as discussed in Chapter 2.

4.4.1.2 Wrist Friction

While under macro-micro control, our ability to reflect forces back to the user is directly limited by friction in the wrist mechanism. During freespace motions, friction in the wrist will be reflected back to the user. If a force scaling factor is used, the frictional forces will be scaled by this factor which, if greater than one, will make freespace motions feel consequently worse. When the slave manipulator makes contact with the environment, forces below the frictional forces in the wrist will not be felt by the user lowering their ability to discriminate contact.

4.4.2 Base Postioner Dynamics

4.4.2.1 Servo Response

The goal of the base positioner is to move the wrist within the body with good postioning bandwidth and accuracy. Any errors in tracking of the master will be perceived as forces by the user and will be felt during freespace motions of the master and slave.

Unlike the wrist, the base positioner does not necessarily need to be light or have particularly low friction. The most important requirement is that its actuators be matched properly to the slave inertia so that it tracks master movements with little error. We should also generate a sufficient overall stiffness to compensate for external disturbance forces such as those caused by the body wall.

4.4.2.2 Structural Dynamics

Structural dynamics should be minimized in order to achieve good position servo response of the base. Also, the overall stiffness of the connection between the master and slave will be limited by the structural stiffness of both the master and the slave.

4.4.2.3 Counterbalancing

Graviationally counterbalancing the slave manipulator, if possible, will help reduce the torques required for the base positioner actuators. It also provides a measure of safety. A counterbalanced slave manipulator will not have a tendency to "fall over" if motor power is lost.

4.5 Sizing

Based on the size of current MIS instruments, the stroke of an instrument into and out of the patient should be roughly 23-25 cm (9-10 in). The depth of penetration into the body should be roughly 33 cm (13 in). The volume of the workspace should be consistent with this. Obviously these values will vary with different size patients and with different procedures, but these give good estimates for a general xsystem.

The size of the instrument shaft must be comparable with current instruments which range from 5 mm diameter to 13 mm diameter. We felt it would be acceptable for the size of this first design to be larger if the potential for miniaturization was reasonably forseeable.

4.6 Force Requirements

I spoke with surgeons in order to generate a specification for x, y, z force levels. Surgeons, unfortunately, have a poor sense of the forces they are applying quantitatively. I performed a simple experiment where I asked a general surgeon[1] to tug on tissue, in this case a pig stomach, using a hand held force sensor with a digital readout and hook attachment (Mark-10, model BG-2). I asked him to tug on the tissue itself, and on suture which was tied into the tissue, "as hard as he might pull during surgery". The range of forces which ranged from 1/2 to 2 lbs. Based on this very rough experiment, I used 2 lbs as a rough specification for desirable x, y, z force capability.

Gripping force is difficult to specify, and yet very important to the ulitmate performance of the system. The primary challenge for the gripper is to hold needles. The problem is that different needle sizes and cross sections, and different needle holder grip surfaces change the required grip force. Typically, smaller needles require less gripping force. Again I performed a simple experiment using a needle holder (Miltex 8-50 with stainless steel, not carbide, grip surfaces). I held one finger loop in a table vise, and held a 3-0 tapered needle with an oval cross section in the jaws by pushing down on the other finger loop through a force sensor (Wagner Force Dial, model FDK 160). This is probably the largest needle I expect to encounter during surgery, so the force required should represent an upper limit. Roughly 2 lbs of force was required on the finger loops to hold the needle "firmly". The needle could wiggle slightly, but to my best estimation was held sufficiently well so as not to roll in the grasp during suturing. After considering the mechanical advantage of the needle holder (the needle was held .75 inches from the pivot point, and the force was applied 4.25 inches from the pivot point), the resulting grip force on the needle was approximately 11.3 lbs.

4.7 Practical Operating Room Constraints

There are a number of issues which to some extent separate from the main design and controls focus of this thesis, but which are critical to the design of an actual product. These issues are discussed below.

[1] Dr. Barry Gardiner of Oakland, CA

4.7.1 Tool Changing

During surgery, many different tools are used. They typically rest in a tray next to the patient, and the surgeon calls for them, to an assistant, as they are needed. The rate at which tools can be interchanged today is high, taking only a few seconds for each tool change.

For a MIS robot to be effective, this cannot change by much. There is nothing intrinsic about the robot which affects the need to change tools quickly. As a result, some distal portion of the robot will have to disconnect and be replaced by alternate versions in order to have needle holders, scissors, tissue graspers, etc. available to the surgeon.

4.7.2 Fit Over Patient

The system must be able to fit over a patient without obstructing other equipment, other surgeons, and surgical assistants. Access to the patient should not be blocked in the event of an emergency. The general system setup is an important issue if such a system is used as a product. These issues include how the system will be mounted in the OR, how it will be positioned above the patient, what happens if the patient is moved or if the OR table is tilted during a procedure.

Different procedures might require completely different positioning of the slaves over the patient. There will likely be two slaves which operate instruments and one slave which positions the endoscopic camera. All will be occupying a limited space compounds the problem of setup and mounting withing the operating room.

4.7.3 Power Sources

The system should use standard power sources which might be available in the operating room. For example, the use of hydraulic or pneumatic compressors would be impractical. Electric motors are a logical choice for operating room use.

4.7.4 Sterilization and Draping

Surgical instruments must of course be sterile. The portion of the slave manipulator which passes into the body must therefore be sterile. This means typically that it may be subject to the heat of an autoclave or to chemical methods of sterilization.

This limits the materials which we may use for the slave and in particular, wrist components.

The entire robot need not be sterilized, since a standard solution already exists which is to cover non sterile systems with sterile drapes. Since the portion of the system which enters the body must be sterile, some sort of interface is required in order to allow the draped non-sterile portion of the robot to connect to a sterile removable instrument while maintaining the sterility of the instrument and transmitting power through the drape. Motions of the robot must be unencumbered by the drape. The design of this interconnection and perhaps of the drape is an issue in itself.

4.8 Safety

The most important specification for a surgical system is that it be safe. Typically a comercial system might have a complex software and digital hardware safety protocol built into the control system to ensure failsafe operation. This would be used in combination with redundant sensors, and brakes or clutches on each axis to prevent uncontrolled motions.

There are also certain mechanical characteristics which we feel make a robot intrinsically safer and which should apply to a system designed for human surgery.

- Counterbalancing of the largest degrees of freedom, either gravitationally or via a spring. This prevents the system from falling under its weight in the event that power is turned off.
- Low link inertia. The energy stored in the system when it is moving is then low. The forces required to dissipate power while stopping a machine can do as much damage to the environment or the machine as forces which the machine can output using its actuators.
- Backdrivability. In the event of a failure, we would like to be able to pull the machine out of the patient under manual control. A simple way to accomplish this is to have backdrivable actuators.

4.9 Summary of Slave Manipulator Goals

To summarize, we have compiled a short list of desirable qualities for a slave manipulator for minimally invasive surgery.

- The system should have at least seven degrees of freedom overall with four outside the body (constrained by the incision point) and the remaining degrees of freedom inside the body in the form of a wrist mechanism and gripper.
- The system should have a compact, slender wrist/shaft which will fit through a cannula inserted in the incision point or at least can be reasonably miniaturized to do so.
- The system should have the ability to orient the wrist 90 degrees relative to the axis of the shaft.
- Wrist singularities, if they exist, should be located at edge of the wrist's range of motion.
- The wrist should allow independent postioning of a point at the tip of the grippers. This redundancy is to enable macro-micro control of the overall system.
- The system should have particularly low inertia in the wrist to enable macro-micro control, but not so low to prevent sufficient servo stiffness from being achieved.
- The system should have particularly low friction in the wrist to enable macro-micro control.
- The system should have a remote center base positioner mechanism which will support the weight of the required motors and wrist unit.
- The base positioner should be designed to have good servo control bandwith.
- The stroke of the instrument into and out of the body should be roughly 8-10", and the overall workspace should also be on this order.
- We should be able to apply 2 lbs in the x, y, z directions.
- We should be able to apply 10 lbs of grip force to hold large needles for suturing.
- A research system should allow tools to be interchanged relatively easily to allow testing of different types of instruments.
- A production system requires that tools be interchanged quickly, within several seconds.
- A productions system must fit over a patient without obstructing other equipment and personel in the operating room.

- A production system must use power sources which are available in the operating room.
- A production system must provide for sterile draping and sterilization of at least the portion which passes through the incision into the human body.
- A production system should be safe to the patient and surgical staff working with it.